

Positivity violations in marginal structural survival models with time-dependent confounding: a simulation study on IPTW-estimator performance

Marta Spreafico

m.spreafico@math.leidenuniv.nl

Mathematical Institute, Leiden University, Leiden 2333 CC, The Netherlands

Department of Biomedical Data Sciences, Leiden University Medical Center, Leiden 2333 ZA, The Netherlands

March 29, 2024

Abstract

In longitudinal observational studies, marginal structural models (MSMs) are a class of causal models used to analyze the effect of an exposure on the (survival) outcome of interest while accounting for exposure-affected time-dependent confounding. In the applied literature, inverse probability of treatment weighting (IPTW) has been widely adopted to estimate MSMs. An essential assumption for IPTW-based MSMs is the positivity assumption, which ensures that each individual in the population has a non-zero probability of receiving each exposure level within confounder strata. Positivity, along with consistency, conditional exchangeability, and correct specification of the weighting model, is crucial for valid causal inference through IPTW-based MSMs but is often overlooked compared to confounding bias. Positivity violations can arise from subjects having a zero probability of being exposed/unexposed (strict violations) or near-zero probabilities due to sampling variability (near violations). This article discusses the effect of violations in the positivity assumption on the estimates from IPTW-based MSMs. Building on the algorithms for simulating longitudinal survival data from MSMs by [Havercroft and Didelez \(2012\)](#) and [Keogh et al. \(2021\)](#), systematic simulations under strict/near positivity violations are performed. Various scenarios are explored by varying (i) the size of the confounder interval in which positivity violations arise, (ii) the sample size, (iii) the weight truncation (WT) strategy, and (iv) the subject's propensity to follow the protocol violation rule. This study underscores the importance of assessing positivity violations in IPTW-based MSMs to ensure robust and reliable causal inference in survival analyses.

Keywords: inverse probability of treatment weighting; marginal structural models; positivity assumption; survival outcome; simulation study.

1 Introduction

In longitudinal observational studies, exposure-affected time-varying confounding represents a specific challenge for estimating the effect of a treatment on the (survival) outcome of interest, as standard analyses fail to give consistent estimators ([Daniel et al., 2013](#); [Clare et al., 2019](#)). In the past decades considerable progresses have been made in developing causal methods for analysing such complex longitudinal data. Marginal Structural Models (MSMs) were introduced as a powerful method, alternatively to structural nested models ([Robins et al., 1992](#)), for confounding control in longitudinal studies ([Robins et al., 2000](#); [Hernán et al., 2000](#); [Williamson and Ravani, 2017](#)). MSMs are models for the *potential* or *counterfactual* outcome that individuals would have experienced if their had received a particular treatment or exposure value. This study focuses on counterfactual time-to-event outcomes by considering marginal structural hazard models (hazard-MSMs) or a discrete-time analogue. The parameters of a MSM can be consistently estimated through various methods, including Inverse Probability of Treatment

Weighting (IPTW) estimators, G-computation, or doubly robust methods (Robins et al., 2000; Clare et al., 2019; van der Laan and Gruber, 2016). Despite less robust, IPTW-based MSMs have largely been adopted in the applied literature, especially in epidemiology and medicine, due to its simplicity in both implementation and interpretation (Clare et al., 2019). IPTW-based MSMs require the correct specification of the exposure model conditional on confounders (i.e., the *weighting model*) and special attention to the identifiability assumptions of consistency, no unmeasured confounding, and positivity (Hernán and Robins, 2020; Cole and Hernán, 2008; Cole and Frangakis, 2009; Williamson and Ravani, 2017). This work focuses on the latter, which is often overlooked compared to confounding bias.

Positivity holds if, for any combination of covariates occurring among individuals in the population, there is a non-zero (i.e., positive) probability of receiving every level of exposure (Cole and Hernán, 2008; Hernán and Robins, 2020). While less well-recognized than bias due to incomplete control of confounding, violations of the positivity assumption can increase both the variance and bias of causal effect estimates (Petersen et al., 2012). Positivity violations can occur in two situations. *Strict* (or *theoretical*) violations occur when it is known that there are subjects with a null probability of being exposed (or unexposed). For example, if according to clinical guidelines certain patients present a contraindication to remaining unexposed, then positivity is violated due to a structural zero probability of not receiving the specific treatment. Even in the absence of structural zeros, *random* zeros may occur by chance due to small sample sizes or highly stratified data by numerous confounders. *Near* (or *practical*) violations refer to situations where the assignment to specific treatment is always theoretically possible but is not observed in the data due to randomness. Sampling variability may indeed result in subjects having a null probability of being exposed (or unexposed) for certain combinations of covariate values.

In the literature, research studies on positivity violations have been previously carried out in a pedagogical manner by using real data to illustrate how incorrect inference occurs in estimating MSMs when positivity is violated (Mortimer et al., 2005; Bembom and van der Laan, 2007; Cole and Hernán, 2008). Findings from different studies agreed that positivity violations have a more severe impact for the IPTW-estimator than other causal estimators. However, when using real data, disentangling the effect of positivity violations from other sources of bias is typically not possible: important confounders may be undetected or unmeasured and the fulfilment of the remaining assumptions underlying the IPTW-estimator is generally difficult to ascertain. Moreover, real data do not allow us to design scenarios that could be of interest, such as studying performance under different sample sizes. To overcome these limitations, other investigations were conducted more systematically by setting up simulation studies (Neugebauer and van der Laan, 2005; Wang et al., 2006; Naimi et al., 2011; Petersen et al., 2012; Léger et al., 2022). Results confirmed that under positivity violations IPTW-estimator performs less well than other methods, becoming very unstable and exhibiting high variability. However, these studies were limited to assessing the causal effect of a treatment assigned either at a single time point or twice.

Despite its importance, the extent to which (near) violations of the positivity assumption impact the IPTW-estimators under different scenarios is not widely understood for a realistic longitudinal survival context. No systematic simulation study exists due to the challenging task of simulating longitudinal survival data under both exposure-affected time-varying confounding and positivity violations. To understand the impact on IPTW-estimators due to positivity violations, it is necessary to disentangle the effect of positivity violations from other sources of bias. The longitudinal simulation setting must hence control over the pathway between confounders and exposure at every point in time. However, even when positivity holds, simulating longitudinal data when the model of interest is a model for potential outcomes, as for MSMs, is generally not straightforward (Evans and Didelez, 2023). The main challenges consist in: (i) replicating the complex dynamics of time-varying confounding; (ii) generating data in such a way that the model of interest is correctly specified; and (iii) in case of survival or other non-collapsible models, reconciling the MSM with the conditional model used in Monte Carlo studies to generate the data. For these reasons, only a few methods for simulating data from MSMs for a survival time outcome have been published in the literature (Xiao et al., 2010; Young et al., 2010; Young and Tchetgen Tchetgen, 2014; Havercroft and Didelez, 2012; Keogh et al., 2021). These algorithms overcome the mentioned issues by imposing restrictions on the data-generating mechanisms, allowing for the correct simulation of longitudinal data from pre-specified MSMs.

The aim and novelty of this work is to develop systematic simulation studies to investigate the impact of positivity violations on the performance of IPTW-estimators in a longitudinal survival context where time-varying confounding is present. Simulation studies play a key role in evaluating the robustness to violation of assumptions, enabling the examination of several properties, such as bias (Morris et al.,

2019; Friedrich and Friede, 2023). The algorithms proposed by Havercroft and Didelez (2012) and Keogh et al. (2021) for simulating longitudinal data from MSMs with a time-varying binary exposure and a survival outcome are extended to incorporate strict and near violations of the positivity assumption. Strict violations are considered in different scenarios by varying the confounder threshold below/above which no subject is unexposed to treatment. Near-violations cases, where not being exposed is rare within certain confounder levels, are studied by incorporating the subject’s propensity to follow or not the violation rule.

This study is organized as follow. Section 2 briefly recalls the notation, MSMs for survival outcomes, and IPTW. Section 3 introduces the designs of the simulation algorithms by Havercroft and Didelez (2012) and Keogh et al. (2021), which are then extended by imposing positivity violations. Section 4 illustrates the results of the simulation studies. R code corresponding to the algorithms and the simulation illustration is provided at <https://github.com/mspreafico/PosViolMSM>. Section 5 finally discusses the findings and provide recommendations.

2 Marginal structural models for potential survival outcomes

2.1 Notation

Let us consider a set of $i = 1, \dots, n$ subjects observed at regular visits $k = 0, 1, \dots, K$ (assumed to be the same for everybody) up until event time $T_i^* = \min(C_i, T_i)$, i.e., the earlier of the time of the actual event of interest T_i and the administrative censoring time C_i . At each visit k , a binary treatment status $A_{i,k} \in \{0, 1\}$ (unexposed vs exposed; control vs treatment) and a set of time-dependent covariates $L_{i,k}$ are observed. A bar over a time-dependent variable indicates the history, that is $\bar{\mathbf{A}}_{i,k} = (A_{i,0}, \dots, A_{i,k})$ and $\bar{\mathbf{L}}_{i,k} = (L_{i,0}, \dots, L_{i,k})$. Finally, the binary failure indicator process is denoted by $Y_{i,k+1}$, where $Y_{i,k+1} = 1$ if subject i has failed (e.g., died) in period $(k; k + 1]$, i.e., $k < T_i \leq k + 1$, or $Y_{i,k+1} = 0$ otherwise.

2.2 Marginal structural models (MSMs) for counterfactual hazard rates

Marginal structural hazards models (hazard-MSMs) are a class of causal models that focus on *counterfactual* time-to-event variables (Hernán et al., 2000; Robins et al., 2000; Hernán and Robins, 2020). These variables represent the time at which an event would have been observed had a patient been administered a specific exposure history $\bar{\mathbf{a}} = (a_0, a_1, \dots, a_K)$ with $a_k \in \{0, 1\}$, which might differ from the actual treatment received $\bar{\mathbf{A}}_i = \bar{\mathbf{A}}_{i,K} = (A_{i,0}, \dots, A_{i,K})$. The *counterfactual event time* that would be observed in a subject under complete exposure history $\bar{\mathbf{a}}$ is denoted by $T^{\bar{\mathbf{a}}}$. Hazard-MSMs hence model the counterfactual hazard rate:

$$\lambda^{\bar{\mathbf{a}}}(t) = \lim_{\Delta \rightarrow 0} \frac{P(t \leq T^{\bar{\mathbf{a}}} < t + \Delta \mid T^{\bar{\mathbf{a}}} \geq t)}{\Delta}. \quad (1)$$

In case of discrete-time hazard of failure, a *marginal structural logistic regression model (logit-MSM)* can be assumed to model the counterfactual probability of failure in a single interval $(k, k + 1]$, given survival up to k . The *logit-MSM* for the counterfactual hazard at visit k is defined as follows:

$$\lambda_k^{\bar{\mathbf{a}}} = \Pr(Y_{k+1}^{\bar{\mathbf{a}}} = 1 \mid Y_k^{\bar{\mathbf{a}}} = 0) = \text{logit}^{-1}[\tilde{\gamma}_0 + g(\tilde{\gamma}_A; \bar{\mathbf{a}}_k)], \quad (2)$$

where $\bar{\mathbf{a}}$ is the the complete treatment strategy, $Y_k^{\bar{\mathbf{a}}}$ is the counterfactual event indicator at visit k , $g(\cdot)$ is a function (to be specified) of the treatment strategy history up to visit k (denoted by $\bar{\mathbf{a}}_k$), and $\tilde{\gamma}_A$ is the vector of log odd ratios.

In the context of continuous-time hazard, the *marginal structural Cox proportional hazard model (Cox-MSM)* form is often assumed to model the counterfactual hazard at time t given treatment history $\bar{\mathbf{a}}$:

$$\lambda^{\bar{\mathbf{a}}}(t) = \lambda_0(t) \exp \left\{ g \left(\tilde{\beta}_A; \bar{\mathbf{a}}_{[t]} \right) \right\}, \quad (3)$$

where $\lambda_0(t)$ is the baseline hazard function, $\bar{\mathbf{a}}_{[t]}$ denotes treatment pattern up to the most recent visit prior to time t (i.e., $[t] = \max_{k \leq t} k$), $g(\cdot)$ is a function (to be specified) of treatment pattern $\bar{\mathbf{a}}_{[t]}$, and $\tilde{\beta}_A$ is a vector of log hazard ratios. Another alternative often used is the *marginal structural Aalen’s additive hazard model (Aalen-MSM)*, defined as

$$\lambda^{\bar{\mathbf{a}}}(t) = \tilde{\alpha}_0(t) + g(\tilde{\alpha}_A(t); \bar{\mathbf{a}}_{[t]}) \quad (4)$$

Table 1: Examples of treatment-pattern forms for function $g(\cdot)$ in Equations (2) to (4).

Form of treatment pattern	Logit-MSM	Cox-MSM	Aalen-MSM
Function $g(\cdot)$	$g(\tilde{\gamma}_A; \bar{\mathbf{a}}_k)$ in (2)	$g(\tilde{\beta}_A; \bar{\mathbf{a}}_{[t]})$ in (3)	$g(\tilde{\alpha}_A(t); \bar{\mathbf{a}}_{[t]})$ in (4)
Current level of treatment	$\tilde{\gamma}_A \cdot a_k$	$\tilde{\beta}_A \cdot a_{[t]}$	$\tilde{\alpha}_A(t) \cdot a_{[t]}$
Duration of treatment	$\tilde{\gamma}_A \cdot \sum_{j=0}^k a_{k-j}$	$\tilde{\beta}_A \cdot \sum_{j=0}^{[t]} a_{[t]-j}$	$\tilde{\alpha}_A(t) \cdot \sum_{j=0}^{[t]} a_{[t]-j}$
Main effect terms at each visit	$\sum_{j=0}^k \tilde{\gamma}_{Aj} \cdot a_{k-j}$	$\sum_{j=0}^{[t]} \tilde{\beta}_{Aj} \cdot a_{[t]-j}$	$\sum_{j=0}^{[t]} \tilde{\alpha}_{Aj}(t) \cdot a_{[t]-j}$

where $\tilde{\alpha}_0(t)$ is the baseline hazard at time t , $\bar{\mathbf{a}}_{[t]}$ denotes treatment pattern up to the most recent visit prior to time t , $g(\cdot)$ is a function (to be specified) of treatment pattern $\bar{\mathbf{a}}_{[t]}$, and $\tilde{\alpha}_A(t)$ is the vector of coefficients at time t .

In the hazard-MSMs (2)-(4), the function $g(\cdot)$ combines information from the treatment pattern up to the most recent visit k prior to time t . Depending on the desired information provided in $g(\cdot)$, the hazard at time t (or visit k) can thus assume a different form. Table 1 shows examples of three forms of the treatment pattern function $g(\cdot)$, specifically: (i) the current level of treatment, (ii) the duration of treatment, or (iii) the history of treatment up to time t through the main effect terms for treatment at each visit. Any other desired form can be alternatively specified.

2.2.1 Hazard-based estimands and counterfactual survival probabilities

The logit-MSM estimates log odd ratios $\tilde{\gamma}_A$, the Cox-MSM the log hazard ratios $\tilde{\beta}_A$, and the Aalen-MSM the cumulative regression coefficients $\int_0^t \tilde{\alpha}_A(s) ds$. Since hazard-based estimands may not have a straightforward interpretation (Keogh et al., 2021), estimates from the MSMs are typically transformed into estimates for an interpretable causal estimand. One example is comparing the counterfactual survival probabilities at time t , i.e., $S^{\bar{\mathbf{a}}}(t) = \Pr(T^{\bar{\mathbf{a}}} > t)$, for *always treated* $\bar{\mathbf{a}} = \mathbf{1} = (1, \dots, 1)$ versus *never treated* $\bar{\mathbf{a}} = \mathbf{0} = (0, \dots, 0)$, or evaluating the marginal risk difference between them. The counterfactual survival probability at time t under treatment history $\bar{\mathbf{a}}$ can be computed based on the different hazard forms:

(i) for the logit-MSMs in (2) is given by

$$S^{\bar{\mathbf{a}}}(t) = \prod_{k \leq t} (1 - \lambda_k^{\bar{\mathbf{a}}}) = \prod_{k \leq t} (1 - \text{logit}^{-1}[\tilde{\gamma}_0 + g(\tilde{\gamma}_A; \bar{\mathbf{a}}_k)]); \quad (5)$$

(i) for the Cox-MSM in (3) is given by

$$S^{\bar{\mathbf{a}}}(t) = \exp\left(-e^{g(\tilde{\beta}_A; \bar{\mathbf{a}}_0)} \int_0^1 \lambda_0(s) ds - \dots - e^{g(\tilde{\beta}_A; \bar{\mathbf{a}}_{[t]})} \int_{[t]}^t \lambda_0(s) ds\right); \quad (6)$$

(iii) for the Aalen-MSM in (4) is given by

$$S^{\bar{\mathbf{a}}}(t) = \exp\left(-\int_0^t \tilde{\alpha}_0(s) ds - \int_0^1 g(\tilde{\alpha}_A(s); \bar{\mathbf{a}}_0) ds \dots - \int_{[t]}^t g(\tilde{\alpha}_A(s); \bar{\mathbf{a}}_{[t]}) ds\right). \quad (7)$$

2.3 Inverse Probability of Treatment Weighting (IPTW)

In the presence of confounders, MSMs can be estimated from the observed data by applying a technique called inverse probability of treatment weighting (IPTW) (Hernán and Robins, 2020). IPTW involves weighting the contribution of each subject i by the inverse of the probability of receiving their actual exposure level given their covariates. This process creates a pseudo-population where confounding is no longer present. To optimize the variance estimation, stabilized (or standardized) weights are usually preferred (Robins et al., 2000; Hernán et al., 2000; Hernán and Robins, 2020; Léger et al., 2022). The stabilized weight for subject i at time t is defined as

$$sw_i(t) = \prod_{k=0}^{[t]} \frac{\Pr(A_{i,k} | \bar{\mathbf{A}}_{i,k-1})}{\Pr(A_{i,k} | \bar{\mathbf{A}}_{i,k-1}, \bar{\mathbf{L}}_{i,k})}, \quad (8)$$

where $\lfloor t \rfloor = \max_{k \leq t} k$ is the largest visit-time prior to t , and A_{-1} is defined to be 0. In the pseudo-population thus created, the effects of time-dependent confounding are balanced, so association in hazard regression models is causation (Hernán and Robins, 2020).

Even when standardized, weights $sw_i(t)$ can largely inflate for a subject i concerned by positivity violation. In such cases, the common approach is to consider truncated stabilized weights $\tilde{sw}_i(t)$ obtained by truncating the lowest and the highest estimations by the 1st and 99th (1-99) percentiles, or alternatively by narrower truncations, such as the 2.5-97.5, 5-95, or 10-90 percentiles (Cole and Hernán, 2008).

2.4 Simulating longitudinal survival data from marginal structural hazard models

Simulating longitudinal data when the model of interest is a model for counterfactual outcomes, as for MSMs, is generally not straightforward (Evans and Didelez, 2023). The main challenges consist in: (i) replicating the complex dynamics of time-varying confounding in the generating mechanism; (ii) generating data in such a way that the model of interest is correctly specified; and (iii) in case of survival or other non-collapsible models, reconciling the MSM with the conditional model used in Monte Carlo studies to generate data. Only a few methods for simulating data from MSMs for a survival time outcome have been published in the literature. These existing algorithms generally impose restrictions on the data-generating mechanisms to overcome the aforementioned issues, allowing for the correct simulation of longitudinal data from pre-specified MSMs. Xiao et al. (2010) and Young et al. (2010) proposed methods for simulating from Cox-MSMs. Havercroft and Didelez (2012) and Young and Tchetgen Tchetgen (2014) outlined how to simulate in a discrete-time setting, from logit-MSMs and discrete-time Cox-MSMs, respectively. These algorithms can be adapted to simulate from a continuous-time Cox-MSM by finely discretizing time. Keogh et al. (2021) introduced a method to simulate from an Aalen-MSM that resulted less-restrictive in the generating mechanism. Recently, Seaman and Keogh (2023) outlined how to simulate from various hazard-MSMs that condition the hazard on baseline covariates.

Among these, the approaches by Havercroft and Didelez (2012) and Keogh et al. (2021) present similar structures of the temporal causal relationships between variables. The directed acyclic graphs (DAGs) in top panels of Figure 1 displays for both cases the assumed data structure and informs which variables, measured at which time points, are confounders of the association between treatment at a given time point and the outcome. Both DAGs are illustrated in discrete-time for a follow-up with $k = 0, \dots, K$ time visits. Variables are assumed to be constant between visits. By imagining splitting the time intervals between successive visits into smaller and smaller intervals, both structures approach the continuous-time setting.

For the current study, these two approaches are used as “truth” benchmarks for cases where longitudinal data generation from the desired hazard-MSM has already been demonstrated and positivity assumption is valid. In Section 3, both are first briefly introduced and then extended by imposing positivity violations.

3 Simulating longitudinal survival data under positivity violations

3.1 Imposing positivity violations

Positivity violations can occur in two scenarios: (i) strict or theoretical violations, where there is null probability of being exposed or unexposed for certain subjects; and (ii) near or practical violations, where sampling variability can lead to subjects having a null probability of being exposed or unexposed for specific combinations of covariate values. To impose strict violations in a data generating mechanism, certain subjects must exhibit a contraindication to being exposed or unexposed.

Let consider that at each time k , there is a contraindication to being unexposed to treatment for subjects presenting a poor health condition. Suppose that this condition is determined by a range of values \mathcal{I}_τ of the confounder $L_{i,k}$. This corresponds to a structurally zero probability that the subject i

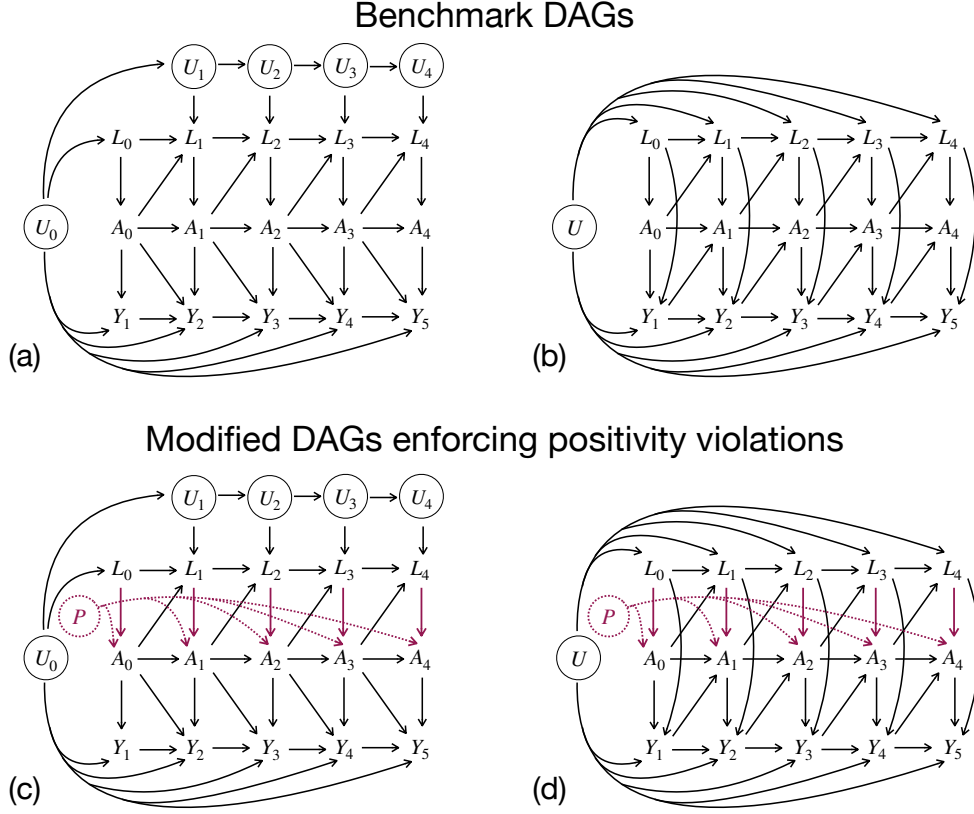


Figure 1: *Top:* Directed acyclic graphs (DAGs) illustrating the temporal causal relationships between variables in the data-generating mechanisms proposed by (a) [Havercroft and Didelez \(2012\)](#) and (b) [Keogh et al. \(2021\)](#). *Bottom:* DAGs illustrating the temporal causal relationships between variables in the proposed data-generating mechanisms under positivity violations.

will be unexposed when $L_{i,k} \in \mathcal{I}_\tau$, that is:

$$\begin{aligned} \Pr(A_{i,k} = 0 \mid L_{i,k} \in \mathcal{I}_\tau, \bar{L}_{i,k-1} = \bar{l}_{k-1}, \bar{A}_{i,k-1} = \bar{a}_{k-1}) &= 0 \quad \text{and} \\ \Pr(A_{i,k} = 1 \mid L_{i,k} \in \mathcal{I}_\tau, \bar{L}_{i,k-1} = \bar{l}_{k-1}, \bar{A}_{i,k-1} = \bar{a}_{k-1}) &= 1 \quad \forall \bar{a}_{k-1}, \bar{l}_{k-1}. \end{aligned} \quad (9)$$

This corresponds to imposing the existence of a protocol rule, whereby subjects are compelled to be exposed at visit k when their health condition is poor, i.e., $L_{i,k} \in \mathcal{I}_\tau \Rightarrow A_{i,k} = 1$ in the data-generating mechanism. The wider the interval \mathcal{I}_τ , the more severe the violation.

Near positivity violations, i.e., violations that can occur by chance, can then be introduced by considering (i) individual propensity P_i to comply with the protocol rule in (9) (i.e., to violate positivity), and (ii) a compliance threshold $\pi \in [0, 1]$. For each subject, a random uniform variable P_i is generated on the interval $[0, 1]$. Subjects with high propensity will be assigned to the positivity non-compliant group, whereas subjects with low propensity to the positivity compliant group. The determination of the groups is established by the compliance threshold π . Specifically, subjects with $P_i \geq \pi$ are considered positivity non-compliant and deterministically assigned to being exposed at time k if their $L_{i,k} \in \mathcal{I}_\tau$. On the other hand, positivity compliant subjects are those with $P_i \leq \pi$, and have a positive probability of receiving every level of the exposure for every value of the confounder $L_{i,k}$. This leads to near-violations of the positivity assumption because, when $L_{i,k} \in \mathcal{I}_\tau$, there are still some exposed and unexposed subjects. The value π can be interpreted as the expected proportion of subjects compliant with positivity, and therefore:

- $\pi = 0 \Rightarrow$ all subjects are non-compliant with positivity \Rightarrow strict positivity violations;
- $\pi = 1 \Rightarrow$ all subjects are compliant with positivity \Rightarrow no positivity violations;
- $0 < \pi < 1 \Rightarrow \pi \times 100\%$ subjects are expected to be compliant with positivity \Rightarrow near positivity violations.

For \mathcal{I}_τ fixed, the higher the compliance threshold π , the less severe the near violation.

By adopting this approach, given an algorithm to simulate longitudinal survival data from MSMs in presence of time-varying confounding, positivity violations can be incorporated by using the pseudocode structure in panel Algorithm 1. The main advantage of imposing positivity violations in an existing approach, where longitudinal data generation from the desired hazard-MSM has already been confirmed, is the ability to directly examine the impact on IPTW estimators solely attributable to positivity violations, rather than other sources of bias. In this way, the original data-generating mechanism can be considered as the “truth” or benchmark case where the positivity assumption holds.

Algorithm 1 General pseudocode for positivity violation.

```

Initialize parameters:  $(\mathcal{I}_\tau, \pi, \dots)$ 
for  $i = 1, \dots, n$  do
  ...
   $P_i \sim \mathcal{U}(0, 1)$  ▷ Draw the individual propensity
  for  $k = 0, \dots, K$  do
     $L_{i,k}$  is assigned based on the generating algorithm
    if  $P_i \geq \pi$  and  $L_{i,k} \in \mathcal{I}_\tau$  then
      exposure is assigned deterministically:  $A_{i,k} = 1$ 
    else
      exposure  $A_{i,k}$  is assigned stochastically based on the generating algorithm
    end if
  ...
end for
end for

```

3.2 Simulation algorithm I

The first algorithm proposed in this work is based on the data-generating mechanism introduced by [Havercroft and Didelez \(2012\)](#) to simulate from a discrete-time logit-MSM. This mechanism is now briefly introduced and then extended by imposing positivity violations.

3.2.1 Benchmark I in a nutshell

Building upon the DAG in panel (a) of Figure 1, [Havercroft and Didelez \(2012\)](#) proposed an algorithm to emulate longitudinal data from the Swiss HIV Cohort Study ([Sterne et al., 2005](#)). The time-dependent binary treatment process $A_{i,k}$ represents exposure to the highly active antiretroviral therapy (HAART) versus no treatment (unexposure). Once HAART has started for a subject i , it continues until failure or end of the follow-up period. The only measured time-dependent confounder $L_{i,k}$ is the non-negative CD4 cell count, measured in *cells*/ μL . Variable $U_{i,k}$ represents the individual general latent health process, indicating a poor individual health status at time k for values close to 0, or good health conditions for values close to 1. The latent process $U_{i,k}$ and the survival process $Y_{i,k+1} \in \{0, 1\}$ are updated at each time point $k = 0, \dots, K$, whereas CD4 cell count $L_{i,k} \geq 0$ and HAART exposure $A_{i,k} \in \{0, 1\}$ are updated very κ -th time points, named check-up visits.

Despite there is no direct arrow from $L_{i,k}$ to $Y_{i,k+1}$, DAG (a) exhibits time-dependent confounding due to $U_{i,0}$ being a common ancestor of \bar{A}_i via \bar{L}_i and \bar{Y}_i . Moreover, $A_{i,k}$ is independent from $\bar{U}_{i,k}$ given $(\bar{L}_{i,k}, \bar{A}_{i,k-1})$ and the vector \bar{L}_i is sufficient to adjust for confounding. The authors hence demonstrated that computing the individual probability of failure in the interval $k < t \leq k + 1$ conditional on survival up to k as

$$\lambda_{i,k} = \text{logit}^{-1} [\gamma_0 + \gamma_{A1} \cdot \{(1 - A_{i,k})k + A_{i,k}K_i^*\} + \gamma_{A2} \cdot A_{i,k} + \gamma_{A3} \cdot A_{i,k}(k - K_i^*)], \quad (10)$$

where K_i^* is the individual treatment initiation time, their procedure correctly simulates data from the following discrete-time logit-MSM:

$$\begin{aligned} \lambda_k^{\bar{a}} &= \text{logit}^{-1} [\tilde{\gamma}_0 + \tilde{\gamma}_{A1} \cdot \{(1 - a_k)k + a_k k^*\} + \tilde{\gamma}_{A2} \cdot a_k + \tilde{\gamma}_{A3} \cdot a_k(k - k^*)] \\ &= \text{logit}^{-1} [\tilde{\gamma}_0 + \tilde{\gamma}_{A1} \cdot d_{1k} + \tilde{\gamma}_{A2} \cdot a_k + \tilde{\gamma}_{A3} \cdot d_{3k}] \end{aligned} \quad (11)$$

where a_k is the binary treatment strategy at time k , k^* is the treatment initiation time, $d_{1k} = \min\{k, k^*\}$ and $d_{3k} = \max\{k - k^*, 0\}$ represent the time elapsed before and after treatment initiation, respectively. The conditional distribution parameters $(\gamma_0, \gamma_{A1}, \gamma_{A2}, \gamma_{A3})$ in (10) are proven to be collapsible with parameters $(\tilde{\gamma}_0, \tilde{\gamma}_{A1}, \tilde{\gamma}_{A2}, \tilde{\gamma}_{A3})$ in the desired logit-MSM (11). Note that $g(\tilde{\gamma}_A; \bar{\mathbf{a}}_k) = \tilde{\gamma}_{A1} \cdot d_{1k} + \tilde{\gamma}_{A2} \cdot a_k + \tilde{\gamma}_{A3} \cdot d_{3k}$ in (11), reflecting that the hazard-MSM depends on a summary of the treatment history rather than only on the current treatment.

3.2.2 Algorithm I: imposing positivity violations in Benchmark I

The first proposed algorithm extends Benchmark I (Section 3.2.1) by imposing positivity violations. As shown in DAG (c) of Figure 1, compared to Benchmark I's structure in DAG (a), two components are introduced: (i) a protocol rule that violates the positivity assumption acting on the purple path $L_{i,k} \rightarrow A_{i,k}$; (ii) the individual propensity $P_i \sim \mathcal{U}(0, 1)$ to follow the positivity violation rule, directly acting on $A_{i,k}$.

Protocol rule. A CD4 count below 500 *cells*/ μL indicates the patient's immune system may be weakened, making them susceptible to developing serious infections from viruses, bacteria, or fungi that typically do not cause problems in healthy individuals. It is hence reasonable to assume that subjects in a poor health condition at time k are identified by $L_{i,k} < \tau$, where $\tau \in [0; 500]$ *cells*/ μL . This is equivalent to a non-negative CD4 range of the form $\mathcal{I}_\tau = [0, \tau)$, where the upper *rule-threshold* τ has to be defined according to the simulation scenario. The higher the τ , the more severe the violations.

Individual propensity. Subjects with propensity P_i above the *compliance-threshold* π (to be defined according to the simulation scenario) are forced to start the treatment as soon as their CD4 count falls below the rule-threshold τ .

Procedure. For each subject $i = 1, \dots, n$, the simulation procedure with K discrete time points and check-ups every κ -th visits is as follows.

1. Generate the individual propensity to follow the violation rule: $P_i \sim \mathcal{U}(0, 1)$.
2. Generate the general latent health status at baseline: $U_{i,0} \sim \mathcal{U}(0, 1)$.
3. Generate the baseline CD4 as a transformation of $U_{i,0}$ by the inverse cumulative distribution function of $\Gamma(3, 154)$ distribution plus an error $\epsilon_{i,0} \sim \mathcal{N}(0, 20)$: $L_{i,0} = F_{\Gamma(3,154)}^{-1}(U_{i,0}) + \epsilon_{i,0}$.
4. If $P_i \geq \pi$ and $L_{i,0} < \tau$, the subject starts HAART and $A_{i,0} = 1$. Otherwise, draw treatment decision $A_{i,0} \sim Be(p_{i,0}^A)$ where $p_{i,0}^A = \text{logit}^{-1}[-0.405 - 0.00405 \cdot (L_{i,0} - 500)]$. If $A_{i,0} = 1$, set the treatment initiation time K_i^* to 0.
5. Compute the conditional individual hazard $\lambda_{i,0}$ for $k = 0$ using (10). If $\lambda_{i,0} \geq U_{i,0}$, death has occurred in the interval $(0, 1]$ and set $Y_{i,1} = 1$. Otherwise, the subject survived and set $Y_{i,1} = 0$.

If the individual is still at risk at visit time $k = 1$:

6. Draw $U_{i,k} = \min\{1, \max\{0, U_{i,k-1} + \mathcal{N}(0, 0.05)\}\}$ as a perturbation of $U_{i,k-1}$ restricted to $[0, 1]$.
7. If k is not a check-up time point, CD4 cell count are not updated and $L_{i,k} = L_{i,k-1}$. Otherwise, update the count as $L_{i,k} = \max\{0, L_{i,k-1} + 150 \cdot A_{i,k-1} + \epsilon_{i,k}\}$, where the addition of 150 indicates the positive effect of exposure to HAART on CD4 count, and the Gaussian drift term $\epsilon_{i,k} \sim \mathcal{N}(100(U_{i,k} - 2), 50)$ implies that the worse is the general health condition $U_{i,k}$ (i.e., value closer to 0), the stronger the negative drift in CD4.
8. If k is not a check-up time point, treatment is not updated and $A_{i,k} = A_{i,k-1}$. Otherwise, assign exposure
 - a. **deterministically:** if $P_i \geq \pi$ and $L_{i,k} < \tau$ or if treatment has started at previous check-up ($A_{i,k-\kappa} = 1$), patient i is exposed to HAART and $A_{i,k} = 1$;

- b. **stochastically:** otherwise, draw treatment decision $A_{i,k} \sim Be\left(p_{i,k}^A\right)$, where $p_{i,k}^A = \text{logit}^{-1}[-0.405 + 0.0205 \cdot k - 0.00405 \cdot (L_{i,k} - 500)]$. The conditional distribution parameters has been set to calibrate the logistic function such that $\Pr(A_{\bullet,0} = 1 \mid L_{\bullet,0} = 500) = 0.4$, $\Pr(A_{\bullet,0} = 1 \mid L_{\bullet,0} = 400) = 0.5$, and $\Pr(A_{\bullet,10} = 1 \mid L_{\bullet,10} = 500) = 0.45$.

If the subject starts the treatment at visit k , set the treatment initiation time K_i^* equal to k .

9. Compute $\lambda_{i,k}$, i.e., the individual probability of failure in the interval $(k; k+1]$ conditional on survival up to k , using (10). If $S_i(t) = \prod_{j=0}^k (1 - \lambda_{i,j}) \leq 1 - U_{i,0}$, the death has occurred in the interval $(k, k+1]$ and $Y_{i,k+1} = 1$. Otherwise, the subject remains at risk and $Y_{i,k+1} = 0$.
10. Repeat steps 6–9 for $k = 2, \dots, K$.

The relative pseudocode is provided in Appendix A. Note that when $\pi = 1$ all subjects are compliant with the positivity assumption and this procedure corresponds to the data generating mechanism of Benchmark I.

3.3 Algorithm II

The second algorithm proposed in this work is based on the data-generating mechanism introduced by Keogh et al. (2021) to simulate from an Aalen-MSM. This mechanism is now briefly introduced and then extended by imposing positivity violations.

3.3.1 Benchmark II in a nutshell

Keogh et al. (2021) proposed a setting where, at each visit $k = 0, \dots, K$, a binary treatment process $A_{i,k} \in \{0, 1\}$ (control vs treatment) and a time-dependent biomarker $L_{i,k} \in \mathbb{R}$ are observed for each subject i . The assumed data structure is illustrated in DAG (b) of Figure 1 using a discrete-time setting where $Y_{i,k+1} = I(k < T_i \leq k+1)$ is an indicator of whether the event T_i occurs between visits k and $k+1$. As the time intervals become very small the algorithm approaches the continuous time setting. The DAG also include a baseline latent variable U_i , representing an subject-specific unmeasured individual frailty, which has a direct effect on $L_{i,k}$ and $Y_{i,k+1}$, but not on $A_{i,k}$.

DAG (b) exhibits time-dependent confounding due to $L_{i,k}$ that predicts subsequent treatment use $A_{i,k}$, is affected by earlier treatment $A_{i,k-1}$, and affects the outcome $Y_{i,k+1}$ through pathways that are not just through subsequent treatment. Moreover, because U_i is not a confounder of the association between the treatment and the outcome, the fact that it is unmeasured does not affect the ability to estimate causal effects of treatments. The author demonstrated that using a conditional additive hazard of the form

$$\lambda_i(t \mid \bar{\mathbf{A}}_{i,[t]}, \bar{\mathbf{L}}_{i,[t]}, U_i) = \alpha_0 + \alpha_A \cdot A_{i,[t]} + \alpha_L \cdot L_{i,[t]} + \alpha_U \cdot U_i, \quad (12)$$

their data generating mechanism correctly simulates data from the additive Aalen-MSM of the form:

$$\lambda^{\bar{\mathbf{a}}}(t) = \tilde{\alpha}_0(t) + \sum_{j=0}^{\lfloor t \rfloor} \tilde{\alpha}_{A_j}(t) \cdot a_{\lfloor t \rfloor - j}, \quad (13)$$

that is an Aalen-MSM including as treatment-pattern $g(\tilde{\alpha}_A(t); \bar{\mathbf{a}}_{[t]})$ the main effect terms at each visit (see Table 1). Researchers using this approach can only specify the parameters $(\alpha_0, \alpha_A, \alpha_L, \alpha_U)$ of the conditional model (12). The true values of the cumulative regression coefficients $C_0(t) = \int_0^t \tilde{\alpha}_0(s) ds$ and $C_{A_j}(t) = \int_0^t \tilde{\alpha}_{A_j}(s) ds$ ($j = 0, \dots, 4$) of the Aalen-MSM (13) must be computed using a simulation-based approach, as detailed in Keogh et al. (2021) (see Section 6.2).

Thanks to the collapsibility property of the Aalen’s additive hazard model, the generating mechanism of Benchmark II does not omit the direct arrow from $L_{i,k}$ to $Y_{i,k+1}$, resulting more realistic in practice compared to Benchmark I. Unlike Benchmark I, which is restricted to generating data closely matching the Swiss HIV Cohort Study (Sterne et al., 2005), Benchmark II can hence be applicable in more general contexts. However, its parameter values need to be carefully selected to ensure that the chance of obtaining a negative hazard, a common drawback in Aalen’s model, is negligible.

3.3.2 Algorithm II: imposing positivity violations in Benchmark II

Analogously to Algorithm I, the second algorithm extends Benchmark II (Section 3.3.1) by imposing positivity violations. As illustrated in DAG (d) of Figure 1, compared to Benchmark II's structure in DAG (b), two components are introduced: (i) a protocol rule that violates the positivity assumption acting on the purple path $L_{i,k} \rightarrow A_{i,k}$; (ii) the individual propensity $P_i \sim \mathcal{U}(0, 1)$ to follow the positivity violation rule, directly acting on $A_{i,k}$.

Protocol rule. Confounder $L_{i,k}$ represents a general biomarker which does not have a direct interpretation in the real world. According to Keogh et al. (2021)'s procedure, the higher the value of $L_{i,k}$ at time k , the higher the probability to be exposed and the hazard. It is hence reasonable to assume that subjects with a poor health condition at time k are identified by $L_{i,k} > \tau$. This is equivalent to a range $\mathcal{I}_\tau = (\tau, \infty)$, where the lower *rule-threshold* τ has to be defined according to the simulation scenario. Here, the lower the threshold τ , the more severe the violation.

Individual propensity. Subjects with propensity P_i above the *compliance-threshold* π (to be defined according to the simulation scenario) are forced to be exposed when their biomarker falls above the rule-threshold τ .

Procedure. For each subject $i = 1, \dots, n$, the simulation procedure with $K + 1$ as administrative censoring time is as follows.

1. Generate the individual propensity to follow the violation rule: $P_i \sim \mathcal{U}(0, 1)$.
2. Generate the individual frailty term: $U_i \sim \mathcal{N}(0, 0.1)$.
3. Generate the baseline biomarker as a transformation of U_i : $L_{i,0} \sim \mathcal{N}(U_i, 1)$.
4. If $P_i \geq \pi$ and $L_{i,0} > \tau$, the subject is exposed to treatment and $A_{i,0} = 1$. Otherwise, draw treatment decision $A_{i,0} \sim Be(p_{i,0}^A)$ where $p_{i,0}^A = \text{logit}^{-1}[-2 + 0.5 \cdot L_{i,0}]$.
5. Event times in the period $0 < t < 1$ are generated by calculating

$$\Delta_i = -\log(v_{i,0})/\lambda_i(t \mid A_{i,0}, L_{i,0}, U_i),$$

where at numerator $v_{i,0} \sim \mathcal{U}(0, 1)$ and the denominator is the individual conditional hazard in (12) with $[t] = 0$ and desired parameters. If $\Delta_i < 1$, death occurred in the interval $t \in (0, 1)$: the event time is set to be $T_i = \Delta_i$ and the failure process is $Y_{i,1} = 1$. Otherwise, subjects with $\Delta_i \geq 1$ remain at risk at time $t = 1$ and set $Y_{i,1} = 0$.

If the individual is still at risk at visit time $k = 1$:

6. Update the biomarker value as: $L_{i,k} \sim \mathcal{N}(0.8 \cdot L_{i,k-1} - A_{i,k-1} + 0.1 \cdot k + U_i, 1)$.
7. Assign exposure
 - a. **deterministically:** if $P_i \geq \pi$ and $L_{i,k} > \tau$, subject i is exposed to treatment and $A_{i,k} = 1$;
 - b. **stochastically:** otherwise, compute $p_{i,k}^A = \text{logit}^{-1}[-2 + 0.5 \cdot L_{i,k} + A_{i,k}]$ and draw treatment decision $A_{i,k} \sim Be(p_{i,k}^A)$.
8. Event times in the period $k \leq t < k + 1$ are generated by calculating

$$\Delta_i = -\log(v_{i,k})/\lambda_i(t \mid \bar{A}_{i,k}, \bar{L}_{i,k}, U_i),$$

where $v_{i,k} \sim \mathcal{U}(0, 1)$ and the denominator is the individual conditional hazard in (12) with $[t] = k$ and desired parameters. If $\Delta_i < 1$, death occurred in the interval $[k, k + 1)$: the event time is set to be $T_i = k + \Delta_i$ and the failure process is $Y_{i,k+1} = 1$. Otherwise, subjects with $\Delta_i \geq 1$ remain at risk at time $k + 1$, i.e., $Y_{i,k+1} = 0$.

9. Repeat steps 6–8 for $k = 2, \dots, K$. Subjects who do not have an event time generated in the period $0 < t < K + 1$ are administratively censored at time $K + 1$.

The relative pseudocode is provided in Appendix B. Note that when $\pi = 1$ all subjects are compliant with the positivity assumption and this procedure corresponds to the data generating mechanism of Benchmark II.

4 Simulation illustration

To analyse the effect of positivity violations on the estimates from the IPTW-based MSMs using Algorithms I and II introduced in Section 3, several investigations were performed by considering various scenarios, as shown in Table 2. Statistical analyses were performed in the R software environment (R Core Team, 2023). Source code is provided at <https://github.com/mspreafico/PosViolMSM>.

Table 2: Parameter specification for different simulation scenarios.

	Algorithm I	Algorithm II
Benchmark^a	$K = 40$ with $\kappa = 5$	$K = 4$ with censoring at $K + 1 = 5$
parameter values	$(\gamma_0, \gamma_{A1}, \gamma_{A2}, \gamma_{A3}) = (-3, 0.05, -1.5, 0.1)$	$(\alpha_0, \alpha_A, \alpha_L, \alpha_U) = (0.7, -0.2, 0.05, 0.05)$
Strict violations		
<i>Settings 1</i>		
sample size:	$n = 100, 300, 500, 800, 1000$	$n = 100, 300, 500, 800, 1000$
rule-threshold:	$\tau = 0, 100, 200, 300, 400, 500$	$\tau = 1, 1.5, 2, 3, 7, 10$
compliance threshold:	$\pi = 0$	$\pi = 0$
weight-truncation:	NoWT	NoWT
<i>Settings 2</i>		
sample size:	$n = 1000$	$n = 1000$
rule-threshold:	$\tau = 0, 100, 200, 300, 400, 500$	$\tau = 1, 1.5, 2, 3, 7, 10$
compliance threshold:	$\pi = 0$	$\pi = 0$
weight-truncation:	NoWT; 1-99; 5-95; 10-90	NoWT; 1-99; 5-95; 10-90
Near violations		
<i>Settings 3</i>		
sample size:	$n = 1000$	$n = 1000$
rule-threshold:	$\tau = 0, 100, 200, 300, 400, 500$	$\tau = 1, 1.5, 2, 3, 7, 10$
compliance threshold:	$\pi = 0.1, 0.3, 0.5, 0.8, 1.0$	$\pi = 0.1, 0.3, 0.5, 0.8, 1.0$
weight-truncation:	NoWT; 1-99	NoWT; 1-99

^aBenchmark parameter values correspond to the values used in the original approach by Havercroft and Didelez (2012) and Keogh et al. (2021).

4.1 Simulation study using Algorithm I

4.1.1 Methods and estimands

As detailed in Table 2, investigations using Algorithm I (Section 3.2.2) were performed in several scenarios by considering various rule-threshold values $\tau \in [0; 500]$ measured in *cells*/ μL (Scenarios I.1, I.2 and I.3), different sample sizes n (Scenarios I.1) and compliance-thresholds $\pi \in [0, 1]$ (Scenarios I.3). The other parameters were set to be identical to those used by Havercroft and Didelez (2012) to consider their results as a benchmark for this analysis. Specifically, $K = 40$ time-points with check-ups every ($\kappa = 5$)-th visit were considered, and the desired conditional distribution parameters in Equation (10) were $(\gamma_0, \gamma_{A1}, \gamma_{A2}, \gamma_{A3}) = (-3, 0.05, -1.5, 0.1)$. In this way, the true values of the parameters in logit-MSM (11) are $(\tilde{\gamma}_0^*, \tilde{\gamma}_{A1}^*, \tilde{\gamma}_{A2}^*, \tilde{\gamma}_{A3}^*) = (-3, 0.05, -1.5, 0.1)$.

The estimands of interest were the regression coefficients $(\tilde{\gamma}_0, \tilde{\gamma}_A)$ and the counterfactual survival probabilities in Equation (5) for the *always treated* versus *never treated* regimens, where $g(\tilde{\gamma}_A; \bar{\mathbf{a}}_k) = \tilde{\gamma}_{A1} \cdot d_{1k} + \tilde{\gamma}_{A2} \cdot a_k + \tilde{\gamma}_{A3} \cdot d_{3k}$. For each regression coefficient, estimated bias and empirical Standard Error (empSE) were considered as performance measures (Morris et al., 2019). For the counterfactual survival, results are presented graphically by showing the mean estimated curves across the $B = 1000$ repetitions.

Note that simulation settings in Scenarios I.3 with $\pi = 1$ and NoWT are equivalent to Benchmark I, regardless of τ (positivity always holds when $\pi = 1$). In such cases, the analyses were based on correctly specified logit-MSMs and correctly specified models for the weights, so the resulting estimates are expected to be approximately unbiased.

4.1.2 Results – Regression coefficients

Figures 2 and 3 displays the estimated performance for $(\hat{\tilde{\gamma}}_0, \hat{\tilde{\gamma}}_{A1}, \hat{\tilde{\gamma}}_{A2}, \hat{\tilde{\gamma}}_{A3})$ in Scenarios I.1 and I.2, respectively. Each line refers to a different value of the rule-threshold τ . The darker the line colour,

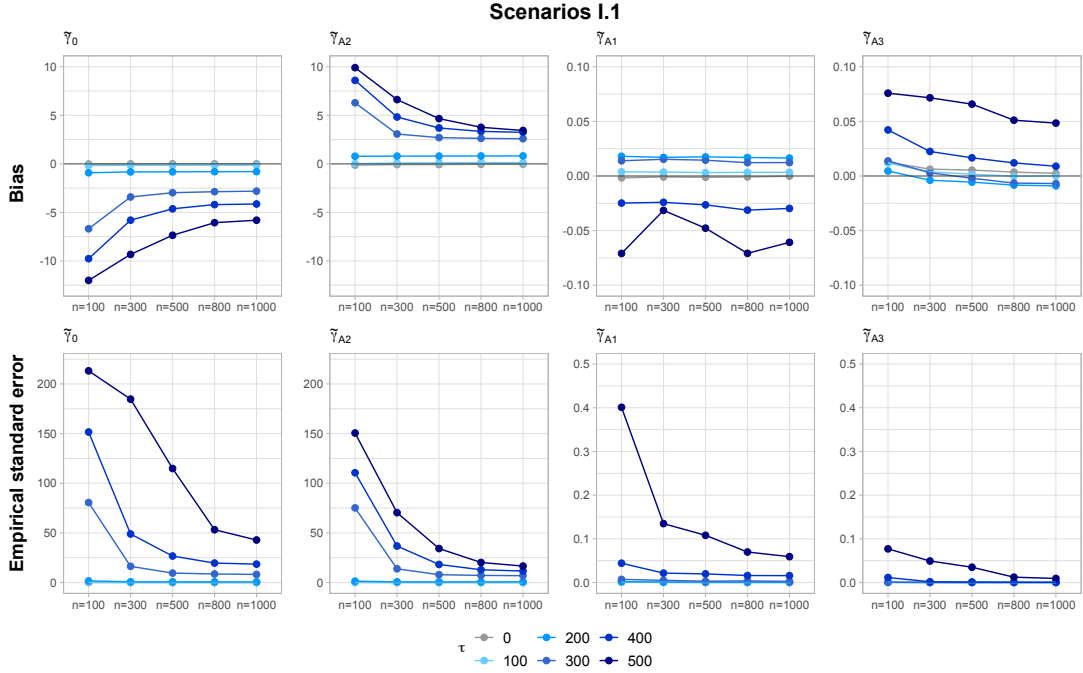


Figure 2: Bias (top panels) and empirical standard error (bottom panels) of the coefficient estimates for the different setting of Scenarios I.1 ($\pi = 0$, No WT). Each column refer to a different coefficient ($\tilde{\gamma}_0$: first column; $\tilde{\gamma}_{A1}$: third column; $\tilde{\gamma}_{A2}$: second column; $\tilde{\gamma}_{A3}$: fourth column). The x-axes show the sample size n . The colours refer to different values of the rule-threshold τ : the darker the colour, the more severe the violation (i.e., the higher τ). Note that the ranges of y-axes differ between $(\tilde{\gamma}_0, \tilde{\gamma}_{A2})$ and $(\tilde{\gamma}_{A1}, \tilde{\gamma}_{A3})$.

the more severe the violation (i.e., the bigger τ). In all scenarios, as the positivity violations become more severe, the absolute bias and the empSE become noticeably larger, especially for $\tilde{\gamma}_0$ and $\tilde{\gamma}_{A2}$ (i.e., the intercept and the parameter most directly related to the effect of exposure). This reflects the fact that severe positivity violations, and the resulting large weights, lead to high variability in the IPTW-based estimates, especially under NoWT. Smaller sample sizes have a higher absolute bias and empSE, as expected (Figure 2). Increasing the sample size indeed mitigates the bias due to finite sample bias, but the bias resulting from the structural positivity violation still persists. Adopting a WT strategy (Figure 3) result in a lower variability and slightly lower bias as extreme weights are truncated, especially for bigger τ . However, compared to WT 1-99, narrowing down the WT did not always lead to better performance.

Similarly, Figure 4 displays the estimated bias and empSE in Scenarios I.3. Under NoWT (solid lines) and fixed τ , the lower the compliance-threshold π , the greater the absolute bias in the results. Compared to the strict positivity violations in Figure 3, near violations led to far less bias and variability, even for low proportion of positivity compliance. All scenarios eventually converge towards a negligible bias as in Benchmark I ($\pi = 1$). In all scenarios, a positivity compliance rate of 80% performed very close to Benchmark I, highlighting that near violations are not as problematic as strict ones in case of low non-compliance rate. Results under 1-99 WT (dotdashed lines) generally show less variability, confirming that WT may help in providing more reliable estimation in case of near-violations, but may result in slightly higher absolute bias.

4.1.3 Results – Counterfactual survival curves

Figure 5 shows the mean counterfactual survival curves, along with the true ones (in orange), in each simulated scenario. Each panel refers to a different (π, WT, n) setting and each line refers to a different τ value. The darker the line colour, the more severe the violation (i.e., the bigger τ). Magnitude and direction of the bias in each parameter determine how closely the estimated counterfactual survival curves match the true (orange) ones. Curves for *never treated* (dashed lines) depend on $(\hat{\gamma}_0, \hat{\gamma}_{A1})$ and therefore generally show a greater deviation compared to those of *always treated* (solid lines) which depend on

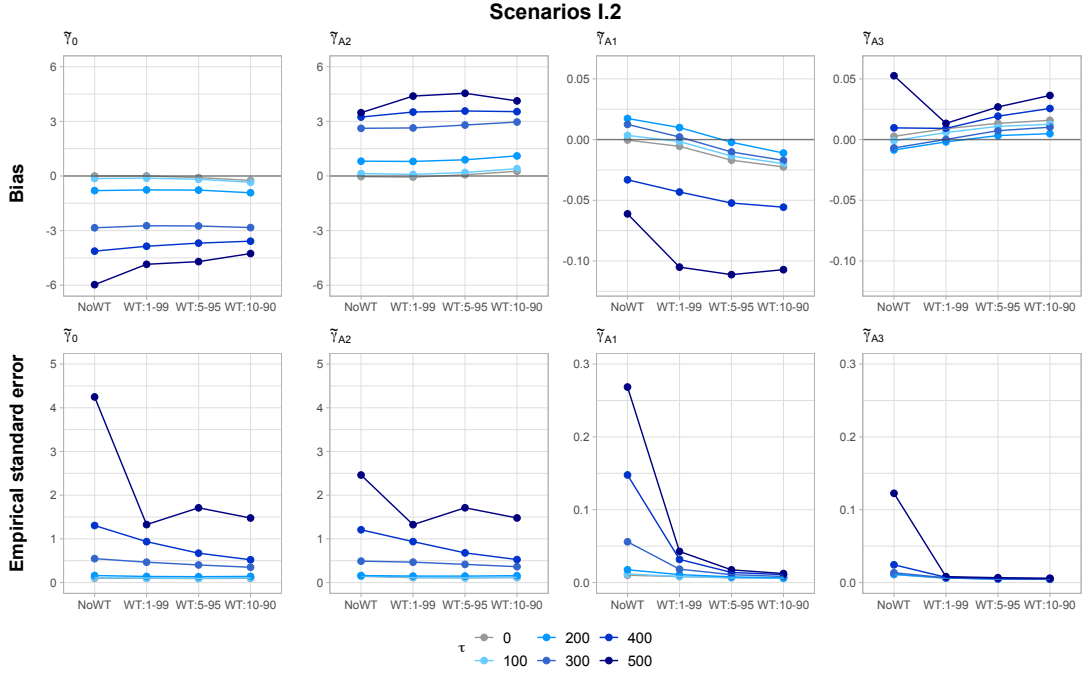


Figure 3: Bias (top panels) and empirical standard error (bottom panels) of the coefficient estimates for the different setting of Scenarios I.2 ($\pi = 0$, $n = 1000$). Each column refer to a different coefficient ($\tilde{\gamma}_0$: first column; $\tilde{\gamma}_{A1}$: third column; $\tilde{\gamma}_{A2}$: second column; $\tilde{\gamma}_{A3}$: fourth column). The x-axes show the Weight Truncation (WT) strategy. The colours refer to different values of the rule-threshold τ : the darker the colour, the more severe the violation (i.e., the higher τ). Note that the ranges of y-axes differ between $(\tilde{\gamma}_0, \tilde{\gamma}_{A2})$ and $(\tilde{\gamma}_{A1}, \tilde{\gamma}_{A3})$.

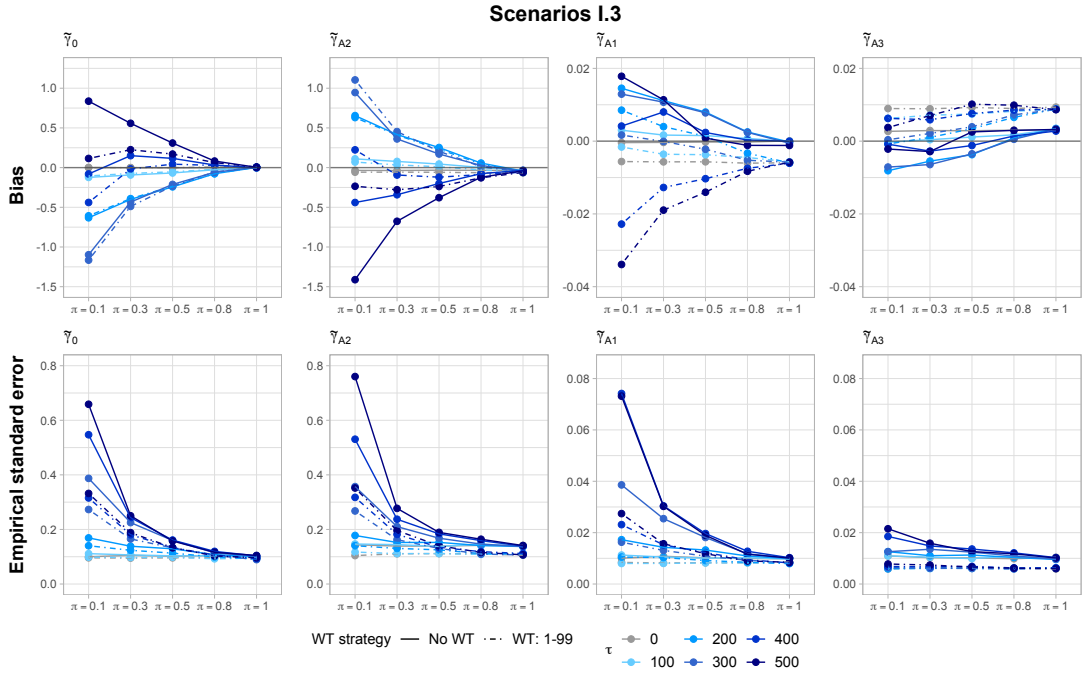


Figure 4: Bias (top panels) and empirical standard error (bottom panels) of the coefficient estimates for the different setting of Scenarios I.3 ($n = 1000$). Each column refer to a different coefficient ($\tilde{\gamma}_0$: first column; $\tilde{\gamma}_{A1}$: third column; $\tilde{\gamma}_{A2}$: second column; $\tilde{\gamma}_{A3}$: fourth column). The x-axes show the compliance-threshold values π . Solid and dotted lines refer to No Weight Truncation (WT) and 1-99 WT strategy, respectively. The colours refer to different values of the rule-threshold τ : the darker the colour, the more severe the violation (i.e., the higher τ). Note that the ranges of y-axes differ between $(\tilde{\gamma}_0, \tilde{\gamma}_{A2})$ and $(\tilde{\gamma}_{A1}, \tilde{\gamma}_{A3})$.

$(\hat{\gamma}_0, \hat{\gamma}_{A2}, \hat{\gamma}_{A3})$. Under strict violations ($\pi = 0$; Scenarios I.1 and I.2), in the *always treated* the negative bias of $\hat{\gamma}_0$ can be balanced by the positive one of $\hat{\gamma}_{A2}$. This is not true for the *never treated* so the deviation notably increases as positivity violations become more severe. Similar behaviours are observed for different sample sizes. Contrary to what it should happen, for more severe violations ($\tau = 300, 400, 500$) being *never treated* result in very good survival, better than the ones for *always treated*. This behavior is accentuated when any WT strategy is employed but it is mitigated by near violations (Scenarios I.3), even for low compliance rates. All scenarios eventually converged to the true values when no positivity violations are present. Accordingly to regression coefficients, near violations resulted in not being as problematic as strict ones. The estimated mean curves are very close to the true ones for an expected positivity compliance rate of 80% under NoWT, or even for 50% under 1-99 WT.

4.2 Simulation study using Algorithm II

4.2.1 Methods and estimands

As detailed in Table 2, investigations were performed in several scenarios by considering different rule-threshold values $\tau \geq 0$ (Scenarios II.1, II.2, II.3), sample size n (Scenarios II.1), and compliance-threshold $\pi \in [0, 1]$ (Scenarios II.3). The other parameters were set to be identical to those considered by Keogh et al. (2021) in order to (i) have the same true values of the estimands of interest for the Aalen-MSM (13) (see Tables 1 and 2 in Keogh et al. (2021)), (ii) use their results as a benchmark for this analysis, and (iii) ensure that the probability of obtaining a negative hazard is negligible for Benchmark II. Specifically, $K = 4$ time-points with administrative censoring at $K + 1$ are considered, and the conditional distribution parameters in Equation (12) were $(\alpha_0, \alpha_A, \alpha_L, \alpha_U) = (0.7, -0.2, 0.05, 0.05)$.

Since $L_{i,k}$ represents a general biomarker without a direct interpretation in the real world, the choice of possible values for τ relied on the distribution of $\{L_{i,k}\}_{k \in \mathcal{K}}$ generated using Benchmark II with $n = 100,000$ subjects. Specifically, the rounded values closest to the 80th, 90th, 95th, 99th, and 100th percentiles (i.e., $\tau = 1, 1.5, 2, 3, 7$) plus an extreme value outside the observed range (i.e., $\tau = 10$) were considered as possible rule-thresholds (see Table 2).

For each scenario, $B = 1000$ simulated datasets were generated. The Aalen-MSM (13) was fitted to each simulated dataset through IPTW estimation using (truncated) stabilized weights. Weight components at time k were estimated by logistic regression models for the probability of being exposed at time k , with numerator and denominators defined as (Keogh et al., 2021)

$$\begin{aligned} \Pr(A_{i,k} = 1 \mid \bar{A}_{i,k-1}, T_i \geq k) &= \text{logit}^{-1}[\theta_0 + \theta_1 \cdot A_{i,k-1}] \\ \Pr(A_{i,k} = 1 \mid \bar{A}_{i,k-1}, \bar{L}_{i,k}, T_i \geq k) &= \text{logit}^{-1}[\theta_0 + \theta_1 \cdot A_{i,k-1} + \theta_2 \cdot L_{i,k}]. \end{aligned}$$

In this way, the denominator model was correctly specified according the data generation mechanism. Various weight truncation (WT) strategies were also explored (Scenarios II.2 and II.3).

The estimands of interest were the cumulative regression coefficients $C_0(t) = \int_0^t \tilde{\alpha}_0(s)ds$ and $C_{A_j}(t) = \int_0^t \tilde{\alpha}_{A_j}(s)ds$ ($j = 0, \dots, 4$), and the counterfactual survival probabilities in Equation (7) for the *always treated* and *never treated* regimens, where $g(\tilde{\alpha}_A(t); \bar{a}_{[t]}) = \sum_{j=0}^{\lfloor t \rfloor} \tilde{\alpha}_{A_j}(t) \cdot a_{[t]-j}$. For the cumulative regression coefficients, results are presented graphically by showing the performance (i.e., bias and empSE) measured at times $t = 1, 2, 3, 4, 5$. For the counterfactual survival curves, the mean value of the estimates across repetitions are presented graphically across time points $t = 1, 2, 3, 4, 5$.

Note that simulation settings in Scenarios II.3 with $\pi = 1$ and NoWT are equivalent to Benchmark II, regardless of τ (positivity always holds). In such cases, the analyses are based on correctly specified Aalen-MSMs and correctly specified models for the weights, so the resulting estimates are expected to be approximately unbiased.

4.2.2 Results – Cumulative regression coefficients

Figures 6 and 7 displays the performance of estimated cumulative coefficient $\hat{C}_{A0}(t)$, i.e., the one related to the current main effect terms, over time $t = 1, 2, 3, 4, 5$ in each simulated scenario. Each line refers to a different value of the rule-threshold τ . The darker the line colour, the more severe the violation (i.e., the lower τ). Smaller sample sizes exhibit a larger absolute bias (Scenarios II.1), as increasing the sample size only mitigates the bias due to the finite sample. In all scenarios, both bias and empSE increase with time. In general, the more severe the violation (darker lines), the worse the performance. Adopting a

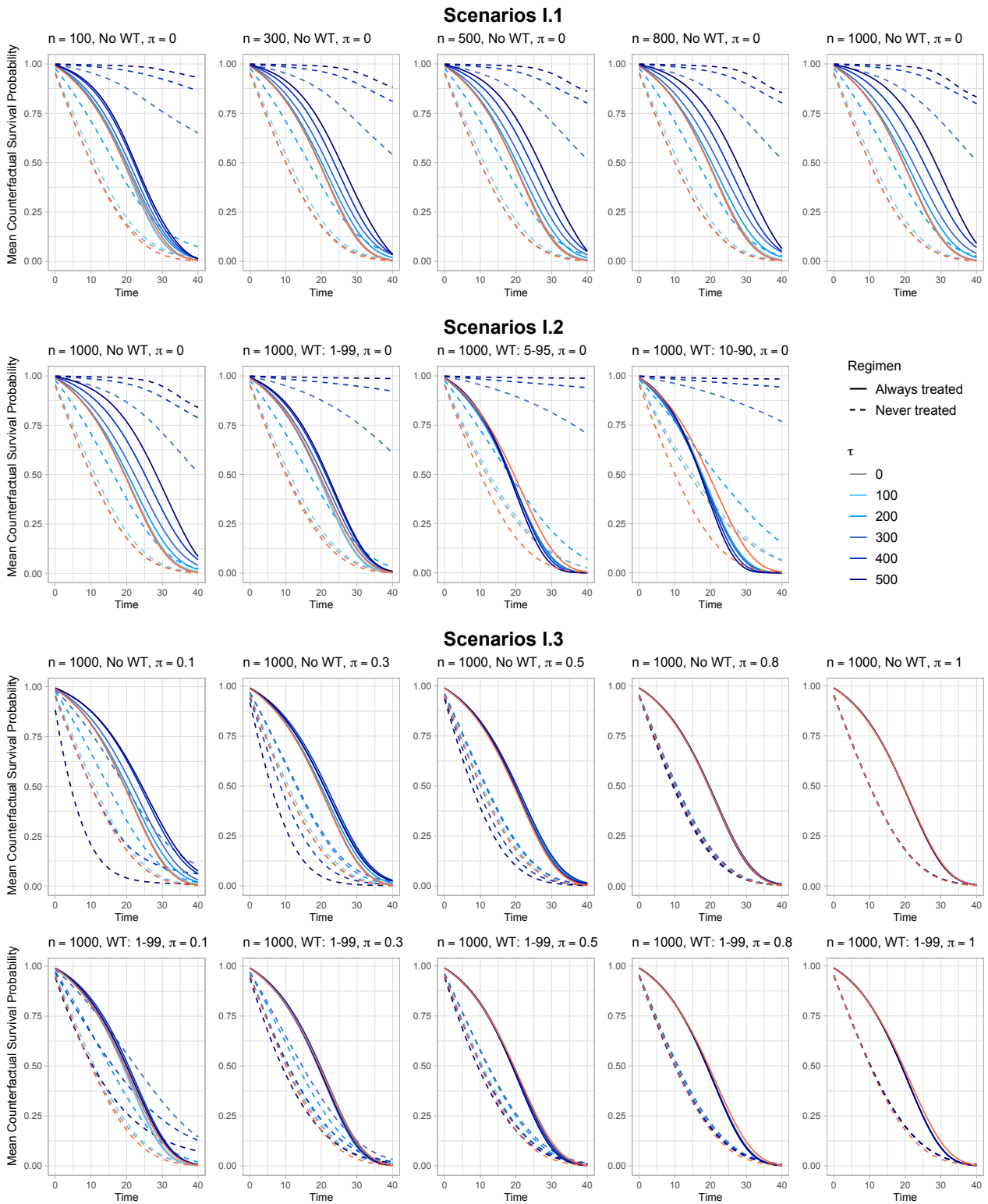


Figure 5: Mean counterfactual survival curves across all the $B = 1000$ repetitions for the different settings of Scenarios I.1, I.2 and I.3. Each panel refers to a different (n, WT, π) setting. Dashed lines refer to the *never treated* regimen, while solid ones to the *always treated* regimen. Curves are colored according to different values of rule-threshold τ . True marginal survival curves are shown in orange.

WT strategy (Scenarios II.2) decreases the empSE, as extreme weights are truncated, especially for more severe violations. However, compared to WT 1-99, narrowing down the WT resulted in worse bias over time. In Scenario II.3, near-violations eventually converged to be unbiased under NoWT, but a small bias still persists under 1-99 WT for $t = 4, 5$. In terms of variability, the empSE are comparable to the one estimated in Benchmark II, even when the expected positivity non-compliance rate is 50%.

Results for the other cumulative coefficients led to similar conclusions: (i) both the estimated absolute bias and the empSE increased with time; (ii) adopting a WT strategy reduces the estimated empSE, but the bias still persists; (iii) under near-violations both bias and empSE eventually converge to the ones estimated for the Benchmark II. The estimated bias for $\hat{C}_0(t)$ is negative and decreases with time. The treatment-related coefficients $\hat{C}_{A_j}(t)$ with $j = 1, 2, 3, 4$ exhibit higher empSE as the violation severity increases. Unlike $\hat{C}_0(t)$ and $\hat{C}_{A_j}(t)$, however, no discernible relationship was found between the values of τ and the resulting bias.

4.2.3 Results – Counterfactual survival probability

Figure 8 shows the mean counterfactual survival curves over times $t = 1, 2, 3, 4, 5$ across repetitions estimated in the various scenarios, along with the true ones (in green). Each panel refers to a different (π, WT, n) setting and each line refers to a different τ value. The darker the line colour, the more severe the violation. These curves can be derived from the cumulative coefficients, whose estimates determine how closely the estimated mean curves match the true (orange) ones. At each time point $t = 1, 2, 3, 4, 5$, the curves for *never treated* (dashed lines) depend solely on $\hat{C}_0(t)$, while all cumulative coefficients contribute to estimating the curves for *always treated* (solid lines). As a result, the estimated mean curves for *never treated* almost always align with the true (green) curves, exhibiting very low bias across time points. Conversely, summing the contributions of each cumulative coefficients leads to higher bias for the *always treated*, especially at later time points.

Small sample sizes (Scenarios I.1) suffered from the main drawback of the additive hazard model, which does not restrict the hazard to be non-negative. This determines survival probabilities for the *always treated* that wrongly increase over time. This issue is mitigated for bigger samples sizes ($n = 800, 1000$). Adopting 1-99 WT (Scenarios II.2 and II.3) improved the performance compared to NoWT. Under near violations (Scenarios II.3), the estimated mean curves correspond to the true ones for an expected positivity compliance rate from 80% upwards under NoWT, or even from 30% under 1-99 WT.

5 Discussion

The positivity assumption requires that each possible treatment occurs with a positive probability in each covariate stratum. This assumption is crucial for valid causal inference but is often overlooked compared to confounding bias. In the context of binary treatment (exposure vs unexposure; treatment vs control), positivity violations can arise from subjects having a zero probability of being exposed/unexposed (strict violations) or near-zero probabilities due to sampling variability (near violations). The existing research literature on positivity violations in MSMs has been limited to examining incorrect inference using real data when positivity is not valid (Mortimer et al., 2005; Bembom and van der Laan, 2007; Cole and Hernán, 2008) or using simulations limited to cases where exposure is assigned either at a single time point or twice (Petersen et al., 2012; Neugebauer and van der Laan, 2005; Wang et al., 2006; Naimi et al., 2011; Léger et al., 2022). Since systematic simulations for a realistic longitudinal-treatment context are still lacking, this study aimed to fill that gap.

Two different algorithms were proposed to simulate data from hazard-MSMs under positivity violations in a survival framework involving binary longitudinal treatment and time-dependent confounding. Systematic simulation studies were conducted to assess the impact of positivity violations on the performance of IPTW-estimators under various scenarios. First, the performance under strict violations was explored by varying the size of the confounder interval $\mathcal{I}\tau$ in which positivity violations arise (i.e., by considering different values of the rule-threshold τ) and the sample size n . Then, observations with extreme weights were resized by truncating the stabilized weights, and estimates for different WT strategies were compared. Finally, near violations of the positivity assumption were addressed by allowing violations to occur within the desired confounder interval $\mathcal{I}\tau$ solely for a proportion $(1 - \pi) \times 100\%$ of subjects non-compliant with the positivity assumption. Different values of π were investigated, along with different WT strategies.

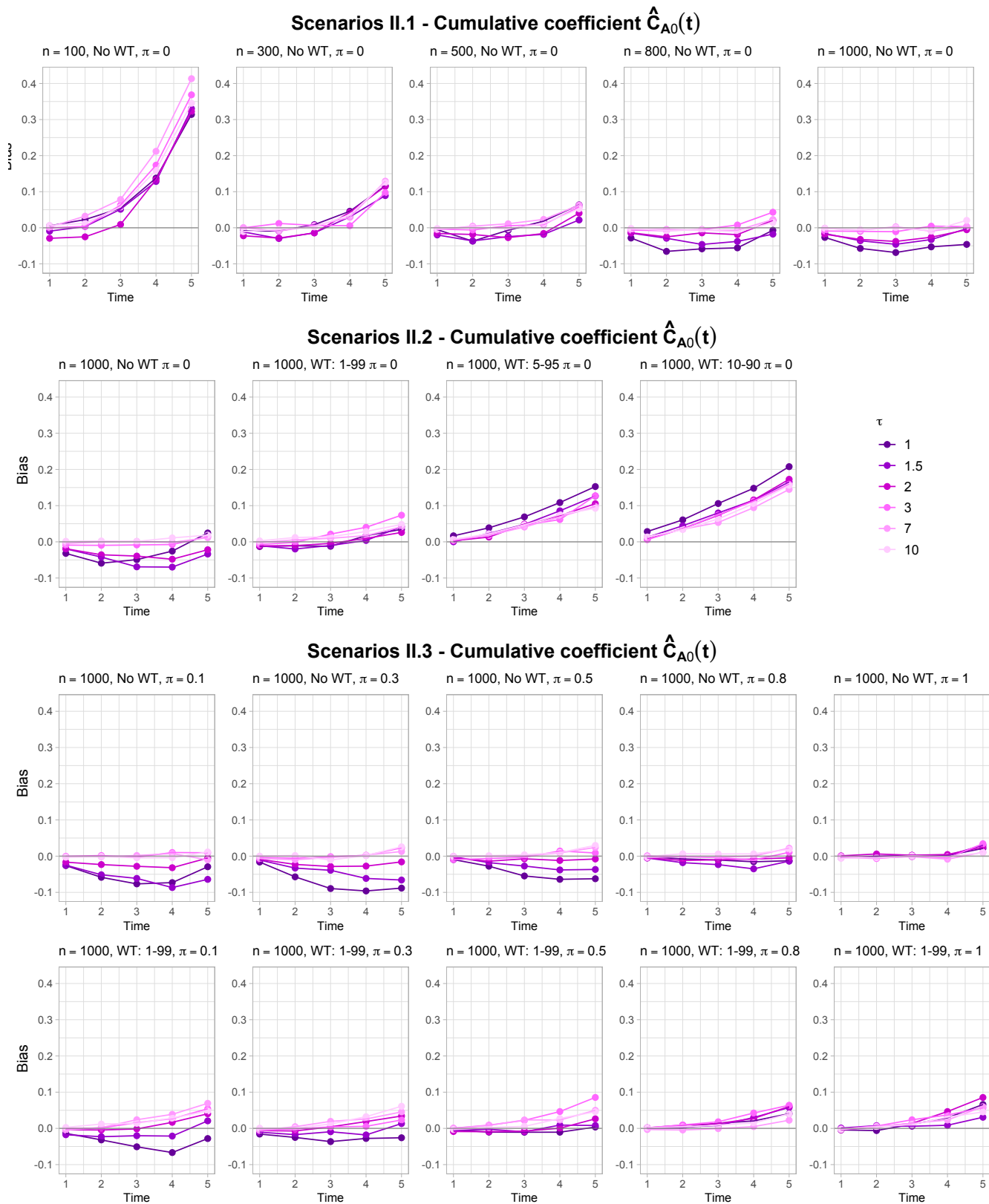


Figure 6: Bias of the estimates for the cumulative coefficient $C_{A0}(t) = \int_0^t \tilde{\alpha}_{A0}(s) ds$ at time points $t = 1, \dots, 5$ under the different settings of Scenarios II.1, II.2 and II.3. Each panel refers to a different (n, WT, π) setting. The colours refer to different values of the rule-threshold τ : the darker the colour, the more severe the violation.

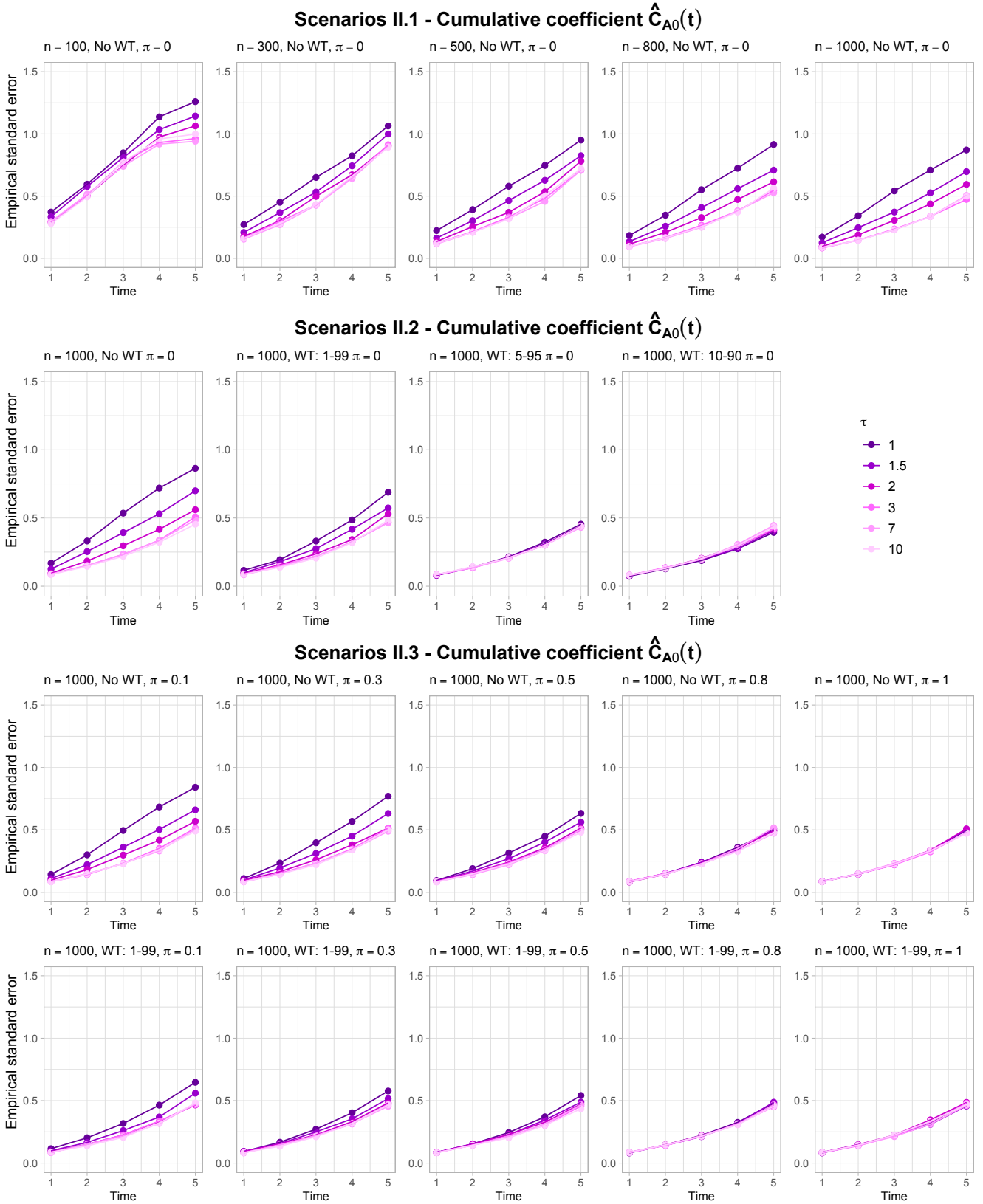


Figure 7: Empirical standard error (empSE) of the estimates for the cumulative coefficient $C_{A0}(t) = \int_0^t \tilde{\alpha}_{A0}(s) ds$ at time points $t = 1, \dots, 5$ under the different settings of Scenarios II.1, II.2 and II.3. Each panel refers to a different (n, WT, π) setting. The colours refer to different values of the rule-threshold τ : the darker the colour, the more severe the violation (i.e., the higher τ).

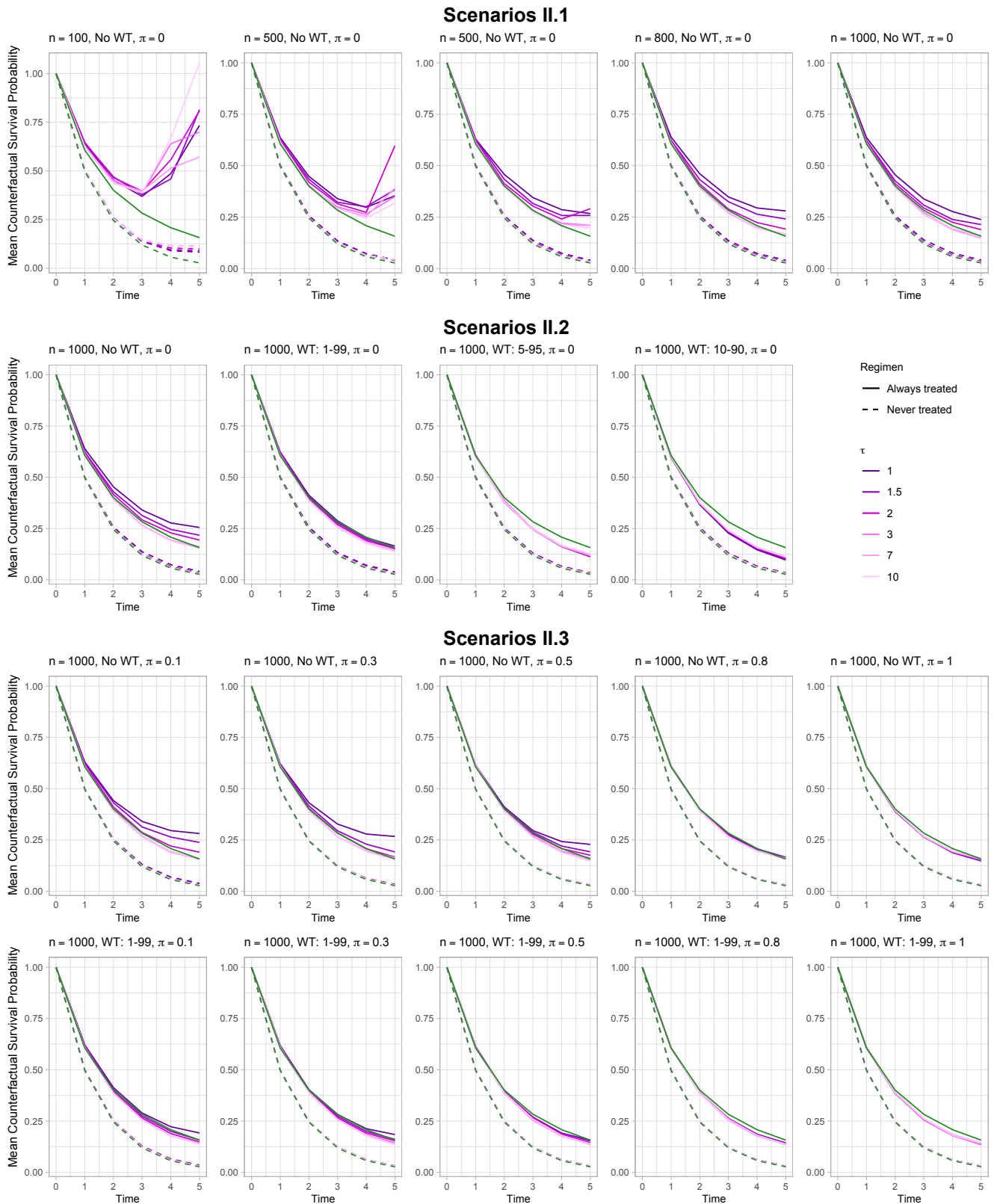


Figure 8: Mean counterfactual survival curves across all the $B = 1000$ repetitions for the different settings of Scenarios II.1, II.2 and II.3. Each panel refers to a different (n, WT, π) setting. Dashed lines refer to the *never treated* regimen, while solid ones to the *always treated* regimen. Curves are colored according to different values of rule-threshold τ . True marginal survival curves are shown in green.

The obtained results suggested that even minor strict violations of the positivity assumption can have significant implications for the performance. Findings from both simulation studies revealed a consistent trend: as the degree of positivity violation becomes more severe (i.e., with larger \mathcal{I}_τ), the performance deteriorates. Increasing the sample size only mitigates the bias and variability due to finite sample bias, while incorrect inference resulting from positivity violations continues to persist. Even when \mathcal{I}_τ is small, the bias of the IPTW-estimator can still be very large due to the presence of large weights, leading to a detrimental impact on the performance. Adopting a WT strategy always decreases variability as extreme weights are truncated, especially for larger \mathcal{I}_τ . However, compared to WT 1-99, narrowing down the WT may not improve the performance in terms of bias. This suggested that bias is the more dominant consideration when the positivity assumption is violated.

Near violations were found to be less problematic than strict violations. Under NoWT, the higher the positivity compliance rate, the better the performance aligns with Benchmark I and II. While variability decreases as violations become milder, no consistent relationship was observed between the width of \mathcal{I}_τ and resulting bias. The decision to adopt the 1-99 WT strategy in near violations must carefully weigh the bias-variance trade-off. Results under the 1-99 WT strategy generally exhibit lower variability, indicating that WT may contribute to more reliable estimations in cases of near-violations. However, this strategy can lead to higher bias, especially for high π values. For high positivity compliance rates ($\pi = 0.8, 1$), NoWT appeared to be generally more favorable than the 1-99 WT strategy, while for intermediate positivity compliance rates ($\pi = 0.3, 0.5$), the opposite was observed.

Algorithm I and II proposed in this work (Sections 3.2.2 and 3.3.2) were built on prior algorithms for simulating longitudinal survival data from MSMs with binary exposures, which were extended to include strict and near violations of positivity. The advantage of extending existing algorithms was threefold. First, the issue of non-collapsibility between conditional and marginal models and the replication of complex confounding dynamics have been already overcome in the original studies. Second, by controlling the exposure-confounder path and avoiding misspecification of the weighting model, the effect due to the imposed positivity violations was separated from other sources of bias. Third, the original Benchmark I and II (Sections 3.2.1 and 3.3.1) were used as the references for the expected true estimates when positivity is valid.

While a direct comparison is not feasible as they pertain to different data-generating mechanisms, Algorithm I generally exhibited poorer performance compared to Algorithm II. This difference may stem from their distinct treatment decision mechanisms. Algorithm I requires continuous exposure until failure or censoring once treatment begins, whereas Algorithm II does not have such a requirement. This constraint limits the possible combinations of treatment-covariate history in Algorithm I, with a significant impact on the estimated coefficients even though very few combinations are missing. Consequently, this influences the estimated mean survival curves, leading to incorrect survival probabilities for the *never treated* group. On the other hand, Algorithm II may suffer from the linear form of the Aalen-MSM, which does not restrict the hazard to be non-negative, resulting in unrealistic survival probabilities.

This work has its limitations, which also open up intriguing possibilities for future research. The way positivity violations was introduced in the algorithms aimed to simulate scenarios where medical guidelines or protocols necessitate exposure when certain confounder values fall within specified ranges. The focus here was on instances where positivity violations occur within a single interval of the confounder variable. However, in real-world scenarios, violations may span varied intervals, suggesting an interesting direction for extending the proposed algorithms. Since this study considered only one continuous confounding variable, another interesting extension would involve incorporating two or more confounders (potentially combining continuous and categorical ones), mirroring practical scenarios where multiple confounding factors are typically present. However, adapting the algorithms to new contexts will require meticulous adaptation. Furthermore, considering the variety of techniques available for estimating causal effects from causal data, future research could explore comparing in a longitudinal setting the performance of the IPTW estimator under positivity violations with that of the doubly robust estimator or the G-computation. Finally, improving the identifiability of parameters in the presence of positivity violations within a longitudinal context remains an unexplored area, presenting a complex challenge for future research. Current methods for addressing positivity violations are primarily designed for point-treatment settings (see [Zhu et al. \(2023\)](#) for an overview), and extending them to a longitudinal framework would introduce significant additional complexity. However, Algorithms I and II developed in this study could serve as valuable tools for evaluating potential new methods developed for this purpose.

In summary, this is the first study investigating how positivity violations impact the IPTW-based esti-

mates from MSMs in a survival framework with longitudinal treatment and time-dependent confounding. In practical analyses, researchers are encouraged to define the causal effect of interest after carefully considering strict positivity violations, remembering that increasing the sample size will not reverse the effect of the violations. While adopting a WT strategy can be appealing in terms of reducing variability, it should be approached cautiously due to the potential risk of increasing the bias. However, when the expected rate of positivity compliance falls within a moderate range, adopting the WT strategy represents a viable compromise for obtaining more reliable estimates. IPTW-based MSMs are widely adopted in applied studies due to their simplicity in both implementation and interpretation. However, analysts must keep in mind that blindly accepting the positivity assumption can have detrimental consequences on the analysis. This work underscores the importance of diligently assessing positivity violations to ensure robust and reliable causal inference in longitudinal survival studies

Acknowledgments. The author wish to thank Prof.dr. Marta Fiocco (Mathematical Institute, Leiden University, Leiden, The Netherlands) for her valuable comments on this work.

References

- Bembom, O. and van der Laan, M. J. (2007). A practical illustration of the importance of realistic individualized treatment rules in causal inference. *Electron. J. Stat.*, 1(none):574–596.
- Bryan, J. (2004). Analysis of longitudinal marginal structural models. *Biostat.*, 5(3):361–380.
- Clare, P. J., Dobbins, T. A., and Mattick, R. P. (2019). Causal models adjusting for time-varying confounding—a systematic review of the literature. *Int. J. Epidemiol.*, 48(1):254–265.
- Cole, S. R. and Frangakis, C. E. (2009). The Consistency Statement in Causal Inference. *Epidemiol.*, 20(3-5).
- Cole, S. R. and Hernán, M. A. (2008). Constructing Inverse Probability Weights for Marginal Structural Models. *Am. J. Epidemiol.*, 168(6):656–664.
- Daniel, R. M., Cousens, S. N., De Stavola, B. L., Kenward, M. G., and Sterne, J. A. (2013). Methods for dealing with time-dependent confounding. *Stat. Med.*, 32(9):1584–1618.
- Evans, R. J. and Didelez, V. (2023). Parameterizing and simulating from causal models. *J. R. Stat. Soc. Series B Stat. Methodol.*, qkad058.
- Friedrich, S. and Friede, T. (2023). On the role of benchmarking data sets and simulations in method comparison studies. *Biom. J.*, page e2200212.
- Havercroft, W. G. and Didelez, V. (2012). Simulating from marginal structural models with time-dependent confounding. *Stat. Med.*, 31(30):4190–4206.
- Hernán, M. and Robins, J. (2020). *Causal Inference: What If*. Boca Raton: Chapman & Hall/CRC.
- Hernán, M. A., Brumback, B., and Robins, J. M. (2000). Marginal structural models to estimate the causal effect of zidovudine on the survival of HIV-positive men. *Epidemiol.*, 11(5):561–570.
- Keogh, R. H., Seaman, S. R., Gran, J. M., and Vansteelandt, S. (2021). Simulating longitudinal data from marginal structural models using the additive hazard model. *Biom. J.*, 63(7):1526–1541.
- Léger, M., Chatton, A., Le Borgne, F., Pirracchio, R., Lasocki, S., and Foucher, Y. (2022). Causal inference in case of near-violation of positivity: comparison of methods. *Biom. J.*, 64(8):1389–1403.
- Morris, T. P., White, I. R., and Crowther, M. J. (2019). Using simulation studies to evaluate statistical methods. *Stat. Med.*, 38(11):2074–2102.
- Mortimer, K. M., Neugebauer, R., van der Laan, M., and Tager, I. B. (2005). An application of model-fitting procedures for marginal structural models. *Am. J. Epidemiol.*, 162(4):382–388.
- Naimi, A. I., Cole, S. R., Westreich, D. J., and Richardson, D. B. (2011). A comparison of methods to estimate the hazard ratio under conditions of time-varying confounding and nonpositivity. *Epidemiol.*, 22(5):718–723.

- Neugebauer, R. and van der Laan, M. J. (2005). Why prefer double robust estimators in causal inference? *J. Stat. Plan. Inference*, 129(1-2):405–426.
- Petersen, M. L., Porter, K. E., Gruber, S., Wang, Y., and van der Laan, M. J. (2012). Diagnosing and responding to violations in the positivity assumption. *Stat. Methods Med. Res.*, 21(1):31–54.
- R Core Team (2023). *R: A Language and Environment for Statistical Computing*. R Foundation for Statistical Computing, Vienna, Austria.
- Robins, J. M., Blevins, D., Ritter, G., and Wulfsohn, M. (1992). G-estimation of the effect of prophylaxis therapy for *Pneumocystis carinii* pneumonia on the survival of AIDS patients. *Epidemiol.*, 3(4):319–336.
- Robins, J. M., Hernán, M. A., and Brumback, B. (2000). Marginal Structural Models and Causal Inference in Epidemiology. *Epidemiol.*, 11(5):550–560.
- Seaman, S. R. and Keogh, R. H. (2023). Simulating data from marginal structural models for a survival time outcome. *arXiv*, 2309.05025.
- Sterne, J. A. C., Hernán, M. A., Ledergerber, B., Tilling, K., Weber, R., Sendi, P., Rickenbach, M., Robins, J. M., Egger, M., and Swiss HIV Cohort Study (2005). Long-term effectiveness of potent antiretroviral therapy in preventing AIDS and death: a prospective cohort study. *Lancet*, 366(9483):378–384.
- van der Laan, M. and Gruber, S. (2016). One-step targeted minimum loss-based estimation based on universal least favorable one-dimensional submodels. *Int. J. Biostat.*, 12(1):351–378.
- Wang, Y., Petersen, M., Bangsberg, D., and van der Laan, M. J. (2006). Diagnosing bias in the inverse probability of treatment weighted estimator resulting from violation of experimental treatment assignment. *U.C. Berkeley Division of Biostatistics Working Paper Series*, Working Paper 211.
- Williamson, T. and Ravani, P. (2017). Marginal structural models in clinical research: when and how to use them? *Nephrol. Dial. Transplant.*, 32(suppl 2):ii84–ii90.
- Xiao, Y., Abrahamowicz, M., and Moodie, E. E. M. (2010). Accuracy of conventional and marginal structural cox model estimators: a simulation study. *Int. J. Biostat.*, 6(2):Article 13.
- Young, J. G., Hernán, M. A., Picciotto, S., and Robins, J. M. (2010). Relation between three classes of structural models for the effect of a time-varying exposure on survival. *Lifetime Data Anal.*, 16(1):71–84.
- Young, J. G. and Tchetgen Tchetgen, E. J. (2014). Simulation from a known cox MSM using standard parametric models for the g-formula. *Stat. Med.*, 33(6):1001–1014.
- Zhu, A. Y., Mitra, N., and Roy, J. (2023). Addressing positivity violations in causal effect estimation using gaussian process priors. *Stat. Med.*, 42(1):33–51.

A Pseudocode of Algorithm I

Algorithm 2 Pseudocode of Algorithm I introduced in Section 3.2.2.

Input parameters:

n = sample size, τ = rule-threshold, π = compliance threshold

K = number of visits, κ = check-up times,

$(\gamma_0, \gamma_{A1}, \gamma_{A2}, \gamma_{A3})$ = conditional distribution parameters in Equation (10)

Algorithm:

for each subject $i = 1, \dots, n$ **do**

$P_i \sim \mathcal{U}(0, 1)$

▷ Individual propensity

$U_{i,0} \sim \mathcal{U}(0, 1)$

$L_{i,0} = F_{\Gamma(3,154)}^{-1}(U_{i,0}) + \epsilon_{i,0}$ where $\epsilon_{i,0} \sim \mathcal{N}(0, 20)$

if $P_i \geq \pi$ and $L_{i,0} < \tau$ **then**

$A_{i,0} = 1$

▷ Deterministic exposure assignment

else

$p_{i,0}^A = \text{logit}^{-1}[-0.405 - 0.00405 \cdot (L_{i,0} - 500)]$

▷ Stochastic exposure assignment

$A_{i,0} \sim \text{Be}(p_{i,0}^A)$

end if

if $A_{i,0} = 1$ **then** $K_i^* = 0$

end if

$\lambda_{i,0} = \text{logit}^{-1}[\gamma_{A0} + \gamma_{A2} \cdot A_{i,0}]$

▷ Conditional hazard (10)

if $\lambda_{i,0} \geq U_{i,0}$ **then** $Y_{i,1} = 1$

else $Y_{i,1} = 0$

end if

$k = 1$

while $Y_{i,k} = 0$ and $k \leq K$ **do**

$U_{i,k} = \min\{1, \max\{0, U_{i,k-1} + \epsilon_{i,k}\}\}$ where $\epsilon_{i,k} \sim \mathcal{N}(0, 0.05)$

if $k \bmod \kappa \neq 0$ **then**

$L_{i,k} = L_{i,k-1}$

$A_{i,k} = A_{i,k-1}$

else

$L_{i,k} = \max\{0, L_{i,k-1} + 150 \cdot A_{i,k-1} + \epsilon_{i,k}\}$ where $\epsilon_{i,k} \sim \mathcal{N}(100(U_{i,k} - 2), 50)$

if $(P_i \geq \pi$ and $L_{i,k} < \tau)$ or $A_{i,k-\kappa} = 1$ **then**

$A_{i,k} = 1$

▷ Deterministic exposure assignment

else

$p_{i,k}^A = \text{logit}^{-1}[-0.405 + 0.0205 \cdot k - 0.00405 \cdot (L_{i,k} - 500)]$

▷ Stochastic exposure assignment

$A_{i,k} \sim \text{Be}(p_{i,k}^A)$

end if

if $A_{i,k} = 1$ and $A_{i,k-1} = 0$ **then** $K_i^* = k$

end if

end if

▷ Conditional hazard (10)

$\lambda_{i,k} = \text{logit}^{-1}[\gamma_0 + \gamma_{A1} \cdot \{(1 - A_{i,k})k + A_{i,k}K_i^*\} + \gamma_{A2} \cdot A_{i,k} + \gamma_{A3} \cdot A_{i,k}(k - K_i^*)]$

if $\prod_{j=0}^k (1 - \lambda_{i,j}) \leq 1 - U_{i,0}$ **then** $Y_{i,k+1} = 1$

else $Y_{i,k+1} = 0$

end if

$k = k + 1$

end while

end for

B Pseudocode of Algorithm II

Algorithm 3 Pseudocode of Algorithm II introduced in Section 3.3.2.

Input parameters:

n = sample size, τ = rule-threshold, π = compliance threshold,

K = number of visits, $(\alpha_0, \alpha_A, \alpha_L, \alpha_U)$ = desired true parameters in Equation 12

Algorithm:

for each subject $i = 1, \dots, n$ **do**

$P_i \sim \mathcal{U}(0, 1)$

▷ Individual propensity

$U_{i,0} \sim \mathcal{N}(0, 1)$

$L_{i,0} \sim \mathcal{N}(U_i, 1)$

if $P_i \geq \pi$ and $L_{i,0} > \tau$ **then**

$A_{i,0} = 1$

▷ Deterministic exposure assignment

else

$p_{i,0}^A = \text{logit}^{-1}[-2 + 0.5 \cdot L_{i,0}]$

▷ Stochastic exposure assignment

$A_{i,0} \sim \text{Be}(p_{i,0}^A)$

end if

$\lambda_i(t | A_{i,0}, L_{i,0}, U_i) = \alpha_0 + \alpha_A \cdot A_{i,0} + \alpha_L \cdot L_{i,0} + \alpha_U \cdot U_i$

▷ Conditional hazard (12)

$\Delta_i = -\log(v_{i,0})/\lambda_i(t | A_{i,0}, L_{i,0}, U_i)$ where $v_{i,0} \sim \mathcal{U}(0, 1)$

if $\Delta_i < 1$ **then** $T_i = \Delta_i$ and $Y_{i,1} = 1$

else $Y_{i,1} = 0$

end if

$k = 1$

while $Y_{i,k} = 0$ and $k \leq K$ **do**

$L_{i,k} \sim \mathcal{N}(0.8 \cdot L_{i,k-1} - A_{i,k-1} + 0.1 \cdot k + U_i, 1)$

if $P_i \geq \pi$ and $L_{i,k} > \tau$ **then**

$A_{i,k} = 1$

▷ Deterministic exposure assignment

else

$p_{i,k}^A = \text{logit}^{-1}[-2 + 0.5 \cdot L_{i,k} + A_{i,k}]$

▷ Stochastic exposure assignment

$A_{i,k} \sim \text{Be}(p_{i,k}^A)$

end if

$\lambda_i(t | \bar{A}_{i,k}, \bar{L}_{i,k}, U_i) = \alpha_0 + \alpha_A \cdot A_{i,k} + \alpha_L \cdot L_{i,k} + \alpha_U \cdot U_i$

▷ Conditional hazard (12)

$\Delta_i = -\log(v_{i,k})/\lambda_i(t | A_{i,0}, L_{i,0}, U_i)$ where $v_{i,k} \sim \mathcal{U}(0, 1)$

if $\Delta_i < 1$ **then** $T_i = k + \Delta_i$ and $Y_{i,k+1} = 1$

else $Y_{i,k+1} = 0$

end if

$k = k + 1$

end while

if $\text{is.null}(T_i)$ **then** $T_i = K + 1$

end if

▷ Administrative censoring at $K + 1$

end for
